Project co-funded by European Union funds (ERDF, IPA)
Project number: DTP3-308-2.3- lifeline MDD

Deliverable D.T1.2.4

Climate Change Study
Climate Change Assessment Report

Author: Imran Nadeem

Date: January 2022

Table of Contents

List of Figures

List of Tables

List of Abbreviations

CC	Climate Change
CCI	Commission for Climatology
CDF	Cumulative Distribution Function
CLIVAR	Climate Variability and Prediction
CORDEX	Coordinated Regional Downscaling Experiment
CMIP5	Coupled Model Intercomparison Project 5
CMIP6	Coupled Model Intercomparison Project 6
DJF	December-January-February
ECA&D	European Climate Assessment & Dataset
EEA	European Environment Agency
EDCDFm	Equidistant cumulative distribution function matching method
ETCCDI	Expert Team on Climate Change Detection and Indices
ESGF	Earth System Grid Federation
EU	European Union
EURO-CORDEX	European Coordinated Regional Downscaling Experiment
GCM	Global Climate Model
JCOMM	The Joint Technical Commission for Oceanography and Marine Meteorology
JJA	June-July-August
JRC	Joint Research Centre
LU	Land Use
MAM	March-April-May
RCM	Regional Climate Model
RCP	Representative Concentration Pathways
SDM	Scale Distribution Mapping
SON	September-October-November
SSP	Shared Socioeconomic Pathways
TBR-MDD	Transboundary Biosphere Reserve Mura-Drava-Danube
UNESCO	United Nations Educational, Scientific and Cultural Organization
WCRP	World Climate Research Programme
WMO	World Meteorological Organization
WWF	World Wide Fund For Nature

I. Introduction

• General Introduction

The present report is the result of a study conducted within the DTP3-308-2.3 lifeline MDD, financed by the European Union´s Interreg Danube Transnational Programme. The area analysed and targeted by the present study (hereinafter called "target area") comprises river sections in the 5-country Biosphere Reserve Mura-Drava-Danube (TBR MDD, Figure 1), shared between Austria, Slovenia, Hungary, Croatia and Serbia. Lower courses of the Drava and Mura Rivers and related sections of the Danube are among Europe's most ecologically important riverine areas. The three rivers form a "green belt" 700 kilometres long, connecting almost 1,000,000 hectares of highly valuable natural and cultural landscapes, including a chain of 13 individual protected areas and 3,000 km2 of Natura 2000 sites. This is the reason why, in 2009, the Prime Ministers of Croatia and Hungary signed a joint agreement to establish the Mura-Drava-Danube Transboundary Biosphere Reserve across both countries. Two years later, in 2011, Austria, Serbia and Slovenia joined this initiative. Together with Croatia and Hungary, the five respective ministers of environment agreed to establish the world's first five-country Biosphere reserve and Europe's largest river protected area. Step by step the TBR MDD was realized: Hungary and Croatia (in 2012), Serbia (in 2017), Slovenia (in 2018) and Austria (2019) achieved UNESCO designation. The pentalateral designation was submitted in 2020 and designation finally achieved in September 2021.

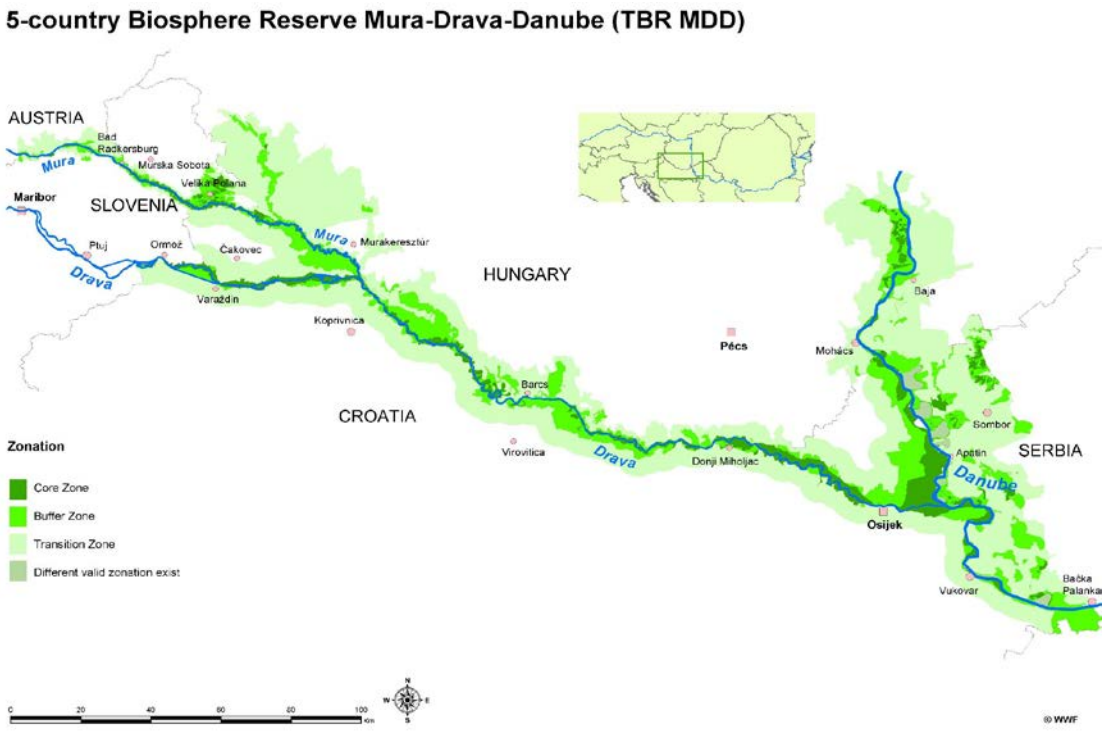

Figure 1 Map of the 5-country Biosphere Reserve Mura-Drava-Danube according to UNESCO designation in September 2021 (WWF Austria)

The project´s work package for Establishing the scientific knowledge base (Work Package T1) has proposed as its aim to establish, as a first, a scientific knowledge base regarding vertical, lateral and longitudinal connectivity within the Mura-Drava-Danube bio-corridor. All studies' results and the overlaid GIS data collected therefore build the basis for a synthesis report on biotic indicators and abiotic framework conditions. This builds the basis for long-term conservation and restoration goals within the 5-country Biosphere Reserve Mura-Drava-Danube (TBR MDD) as well as for formulation of a TBR MDD River Restoration Strategy, elaborated in the framework of the same project (Output OT2.4). The facts and results presented in this project therefore come from a first ever such scientific assessment, harmonized on a 5-country scale, setting the ground for future decision-making on 5-country level on river management and restoration. Whereas such activities and knowledge in each of the countries involved in the TBR MDD partly exist, this was the first time methods and area were harmonized for monitoring and studies of the biotic elements and the abiotic framework conditions for the Mura-Drava-Danube river corridor.

- **Problem Statement**

The Mura-Drava-Danube floodplain spans five countries and provides various important functions for the local population such as fresh water, flood protection and suitable soil conditions for agriculture. The climate projections indicate that every populated basin in the world will experience changes in river discharge and many will experience water stress (Palmer et al., 2008). For example, a recent Join Research Center (JRC) assessment of the future water resources of the Danube River Basin finds that climate change beyond 2°C would result in increased flooding and water stress, remarkably drier summer months and significant flood damage in cities along the Danube River and its tributaries (Bisselink et. al. 2018). Similarly, climate change is expected to increase contrasts between climate zones resulting in significant changes in river discharge of the Drava-Mura catchment (Lóczy D., 2019). The TBR MDD needs management action to mitigate the impacts of climate change through the quantification of climate change and its impact on health, water resources and biodiversity. The study area is vulnerable to the projected changes in climate. Predictions of a warmer climate and changes in precipitation patterns would strongly affect wetland ecological functions through changes in hydrology, biogeochemistry, and biomass accumulation.

The climate change report is meant to provide climate change projections of temperature and precipitation along with changes in extremes, up to year 2100 based on a multi-model ensemble of regional climate models using two future scenarios.

- **State of Knowledge**

The River Danube which has the second largest catchment area in Europe has always been of great interest in the scientific community. As the river flows through ten European countries, most of the research is done on a regional level (Bertalanič et. al. 2019 and Pongracz et. al. 2011). Moreover, there are several studies on continental level

which evaluate impacts of climate change on river flow regimes in Europe (Schneider et. al. 2013, Lobanova et al., 2018 and Theobald et al., 2020). Yet there is not much done in terms of climate change projection and quantification of extremes, based on a multi-model ensemble of regional climate models for the TBR MDD. Most of the studies done in recent years focus on the main Danube region (e.g., Klein et al., 2012 Stagl et. al. 2015) and do not give much insight into the impact of climate change on a local scale for the Mura-Drava-Danube floodplains. In the light of above, the present study is one of its kind highlighting the effects of climate change and its impact on hydrology and biodiversity of the region using the output of state-of-the-art regional climate models.

- ### Study Aims

The aim of the study is to analyze the data of existing regional climate model projections for the TBR MDD up to year 2100 using two future emission scenarios RCP4.5 and RCP8.5. The goal is to select five models for each emission scenario for multi-model climate change assessment. The downscaled and bias-corrected data of selected RCMs is used to derive the future climate change signals of temperature and precipitation. Moreover, temperature and precipitation related climate extremes are calculated and changes in extreme events under future warming climate are presented. The findings and data of this study are useful for the impact modelling in different sectors, which will serve as an input for climate risk assessment and vulnerability and adaptation analysis for TBR MDD. Provision of data to water and hydrological assessment and providing recommendations are also part of the current study.

II. Methodology

- ### Overview

In this study, climate change assessment is carried out based on a multi-model ensemble of bias-corrected regional climate scenarios for the 5-country Biosphere Reserve Mura-Drava-Danube and surrounding areas to account for the climate change in the catchment areas of the river in TBR MDD. The scope of work includes the following tasks:

- retrieve and analyze data of regional climate simulations carried out in WCRP European Coordinated Regional Downscaling Experiment (EURO-CORDEX) provided by Earth System Grid Federation (ESGF);
- analyze the historical and future temperature and precipitation for TBR MDD to select most suitable five regional climate models (RCMs) for each scenario (RCP4.5 & RCP8.5);
- downscale and bias-correct the daily data of selected RCMs against the gridded observation E-OBS data from European Climate Assessment & Dataset (ECA&D)
- validate the bias-corrected data and calculate the climate change signals for temperature and precipitation in future periods;
- calculate climate extreme indices from bias-corrected data and quantify the changes in extreme events in future periods under different scenarios.

Analysis is done on monthly, seasonal, and annual basis, and also for four time periods namely 1976-2005 (reference period), 2021-2050 (near future), 2036-2065 (mid-century) and 2071-2100 (end-century). For the ensemble-based analysis, a given parameter or climate indicator is calculated for each individual model before taking the ensemble mean.

- ## Observed and Model Datasets

In the present study, different data sources are used and analyzed. A brief overview of the dataset used is given below. All the datasets used in the study are freely available.

E-OBS gridded Observations

The bias-correction and validation of regional climate model output requires gridded observational datasets. For this purpose, the E-OBS dataset is used. It is a daily gridded land-only observational dataset that covers the European region and is constructed from the interpolation of station-derived meteorological observations by the ECA&D initiative (Klein Tank et al., 2002). The latest version of E-OBS (ver. 23.1) used in this study is an improved version based on the ensemble approach described by Cornes et al., 2018. The E-OBS data has a horizontal resolution of 0.1° x 0.1° (hereafter EOBS-0.1) and is available from 1950 till present. The daily data of precipitation, minimum temperature and maximum temperature is used. The literature clearly states that the presented accuracy of E-OBS data is relatively high, particularly in the case of temperature fields, and it can be used as proxies for observations to bias-correct and even as input for hydrological models, especially in regions with limited meteorological stations (Lazoglou, G et. al. 2019). The topographic elevation of E-OBS is shown in figure 2.

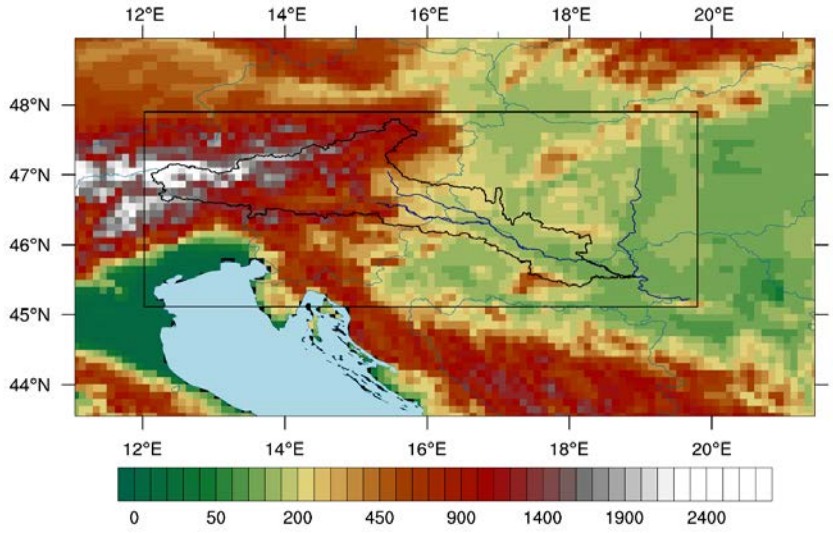

Figure 2 Geographical domain showing topographic elevation of E-OBS gridded dataset. The climate data is downscaled to this domain; however, the analysis is done for the area highlighted with a rectangular box. (Drava River basin is also outlined)

Regional Climate Model Data

To assess the range of potential future climate change in the TBR-MDD, the data of regional climate models (RCMs) from the latest set of the Coordinated Regional Downscaling Experiment (CORDEX) of the World Climate Research Programme (WCRP) is used. The CORDEX provides an internationally coordinated framework to improve regional climate scenarios. This includes harmonization of model evaluation activities and the generation of multi-model ensembles of regional climate projections for the land-regions worldwide. As part of the global CORDEX framework, the EURO-CORDEX initiative (www.euro-cordex.net) provides regional climate projections for Europe at 12.5 km (EUR-11) resolution, thereby complementing coarser-resolution data sets of former activities like EU Projects PRUDENCE and ENSEMBLES.

Out of total 46 GCM-RCM combinations available at EURO-CORDEX database, we used data from 18 EUR-11 Regional Climate Model (RCM) simulations, for which data is available for two selected representative concentration pathway scenarios at +4.5 W/m2 and +8.5 W/m2. The selected regional climate models along with driving GCMs are presented in Table 1. The representative concentration pathway 4.5 (8.5) specifies concentrations of greenhouse gasses that will result in a total radiative that delivers global warming at an average of 4.5 (8.5) watts per square meter across the planet. The RCP4.5 pathway is considered a mid-range scenario and delivers a global temperature increase of about 2.4˚C by 2100, relative to pre-industrial temperatures. The RCP8.5 is a high emission scenario which would deliver a total global warming of about 4.3˚C by 2100.

Table 1 List of 18 regional climate models used for initial analysis to select the five best performing regional climate models for the study area.

No.	Driving Global Climate Model (GCM)	Regional Climate Model (RCM)	Abbreviation
1	NCC-NorESM1-M	SMHI-RCA4_v1	NorESM1_M-SMHI_RCA4
2	NCC-NorESM1-M	GERICS-REMO2015_v1	NorESM1_M-GERICS_REMO
3	NCC-NorESM1-M	DMI-HIRHAM5_v3	NorESM1_M-DMI_HIRHAM5
4	MPI-M-MPI-ESM-LR	SMHI-RCA4_v1a	MPI_ESM_LR-SMHI_RCA4
5	MPI-M-MPI-ESM-LR	MPI-CSC-REMO2009_v1	MPI_ESM_LR-MPI_CSC_REMO
6	MPI-M-MPI-ESM-LR	CLMcom-CCLM4-8-17_v1	MPI_ESM_LR-CLMcom_CCLM4
7	MOHC-HadGEM2-ES	SMHI-RCA4_v1	HadGEM2_ES-SMHI_RCA4
8	MOHC-HadGEM2-ES	KNMI-RACMO22E_v2	HadGEM2_ES-KNMI_RACMO22E
9	MOHC-HadGEM2-ES	DMI-HIRHAM5_v2	HadGEM2_ES-DMI_HIRHAM5
10	MOHC-HadGEM2-ES	CLMcom-CCLM4-8-17_v1	HadGEM2_ES-CLMcom_CCLM

11	IPSL-IPSL-CM5A-MR	SMHI-RCA4_v1	IPSL_CM5A_MR-SMHI_RCA4
12	ICHEC-EC-EARTH	KNMI-RACMO22E_v1	EC_EARTH-KNMI_RACMO22E
13	CNRM-CERFACS-CNRM-CM5	SMHI-RCA4_v1	CNRM_CM5-SMHI_RCA4
14	CNRM-CERFACS-CNRM-CM5	RMIB-UGent-ALARO-0_v1	CNRM_CM5-UGent_ALARO
15	CNRM-CERFACS-CNRM-CM5	KNMI-RACMO22E_v2	CNRM_CM5-KNMI_RACMO22E
16	CNRM-CERFACS-CNRM-CM5	CNRM-ALADIN63_v2	CNRM_CM5-CNRM_ALADIN63
17	CNRM-CERFACS-CNRM-CM5	CNRM-ALADIN53_v1	CNRM_CM5-CNRM_ALADIN53
18	CNRM-CERFACS-CNRM-CM5	CLMcom-CCLM4-8-17_v1	CNRM_CM5-CLMcom_CCLM

- ## Selection of Best Performing RCMs

This section describes the selection of the five most suitable models for each RCP4.5 and RCP8.5 from the initially selected 18 models highlighted in Table 1. Climate models are often selected based on their skill to simulate the present and near-past climate. This approach is referred to as the past-performance approach. The decision on which variables are considered, depends on the character and goals of the climate change impact assessment. For the present study, the most common variables i.e., temperature and precipitation, are considered as the most relevant ones. To select the better performing models over the TBR MDD, we use the scatter plot of changes in temperature versus changes in precipitation (delta-T and delta-P approach). The selection is based on the following criteria:

criteria:

- **Availability:** The selected model should have daily data available for minimum and maximum temperature, and daily precipitation data for both RCP scenarios. The models with missing data are excluded.
- **Representation of Historical Climate (Garbage in – Garbage out):** The selected model should correctly represent the annual cycle and long-term climatological means over the study period. The bias-correction methods correct the biases in the model but a model with incorrect annual cycle cannot be corrected with significant accuracy. All models show correct representation of monthly mean temperature (30-year monthly mean climatology compared with E-OBS), but some models don't reproduce the precipitation annual cycle correctly. Figure 3 shows the normalized monthly errors in precipitation as compared to observations (E-OBS) over the study region (shown in Figure 2) for the period 1976-2005. It is noted that NorESM1_M-SHMI_RCA4 and HadGEM2_ES-CLMcom_CCLM show significant wet-biases in winter and strong underestimation of precipitation in summer months. All models with a sum of absolute monthly errors above 0.2 are excluded.

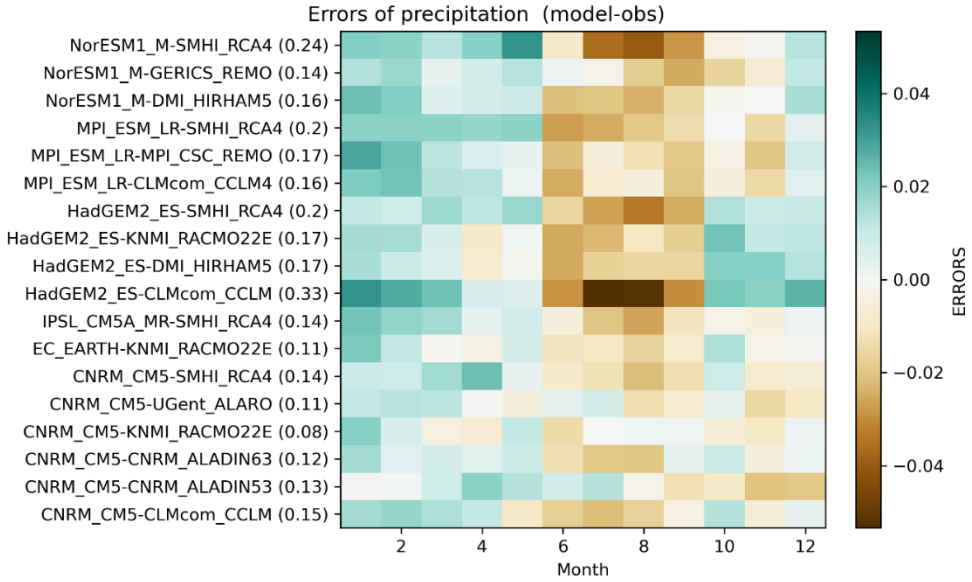

Figure 3 Normalized monthly errors in simulated precipitation as compared to E-OBS calculated from monthly climatological means for the reference period 1976-2005

- **Interannual Variability**: The interannual variability of all 18 models and E-OBS is plotted in Figure 4 below. The figure shows the box and whisker plots of normalized annual precipitation. The annual precipitation sums are normalized with climatological means and variability across the years (1976-2005) is presented. The models with significantly higher variability (0.13 and above) than observations (0.11) are excluded.

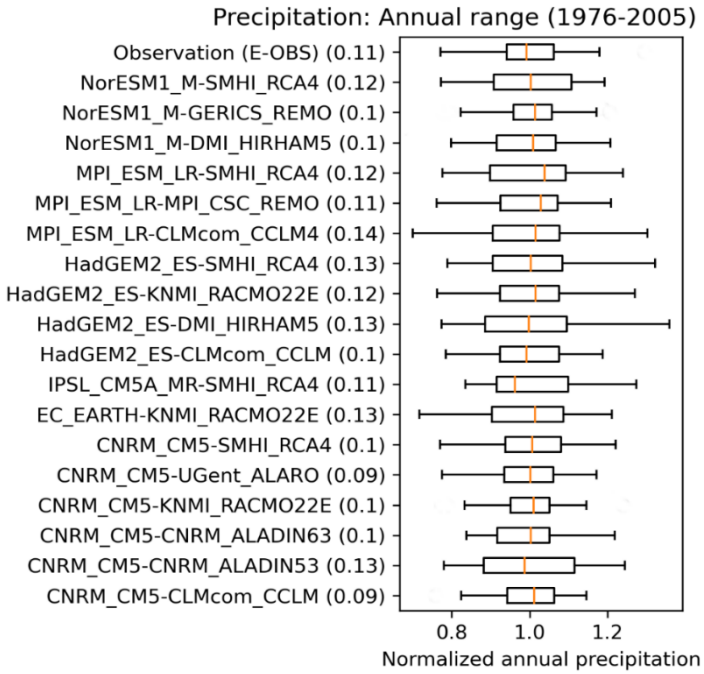

Figure 4 Interannual variability calculated from normalized annual precipitation for the period 1976-2005. The models with very high interannual variability are excluded in the selection process.

- **Temperature Vs Precipitation Climate Change Scatter plot**: To select models which represent the full spectrum of climate change in terms of both temperature and precipitation change, the climate change signals (CC-signals) for the period 2071-2100 from the base period 1976-2005 are calculated. The CC-signals of temperature (absolute change in °C) and CC-signals of precipitation (relative fraction) from 18 models and ensemble mean are shown in Figure 5 for RCP4.5 (above) and RCP8.5 (below). The ensemble mean is shown with black diamond markers. Skipping all the models which don't fulfil the above three criteria, the five models shown in Table 2 are finally selected.

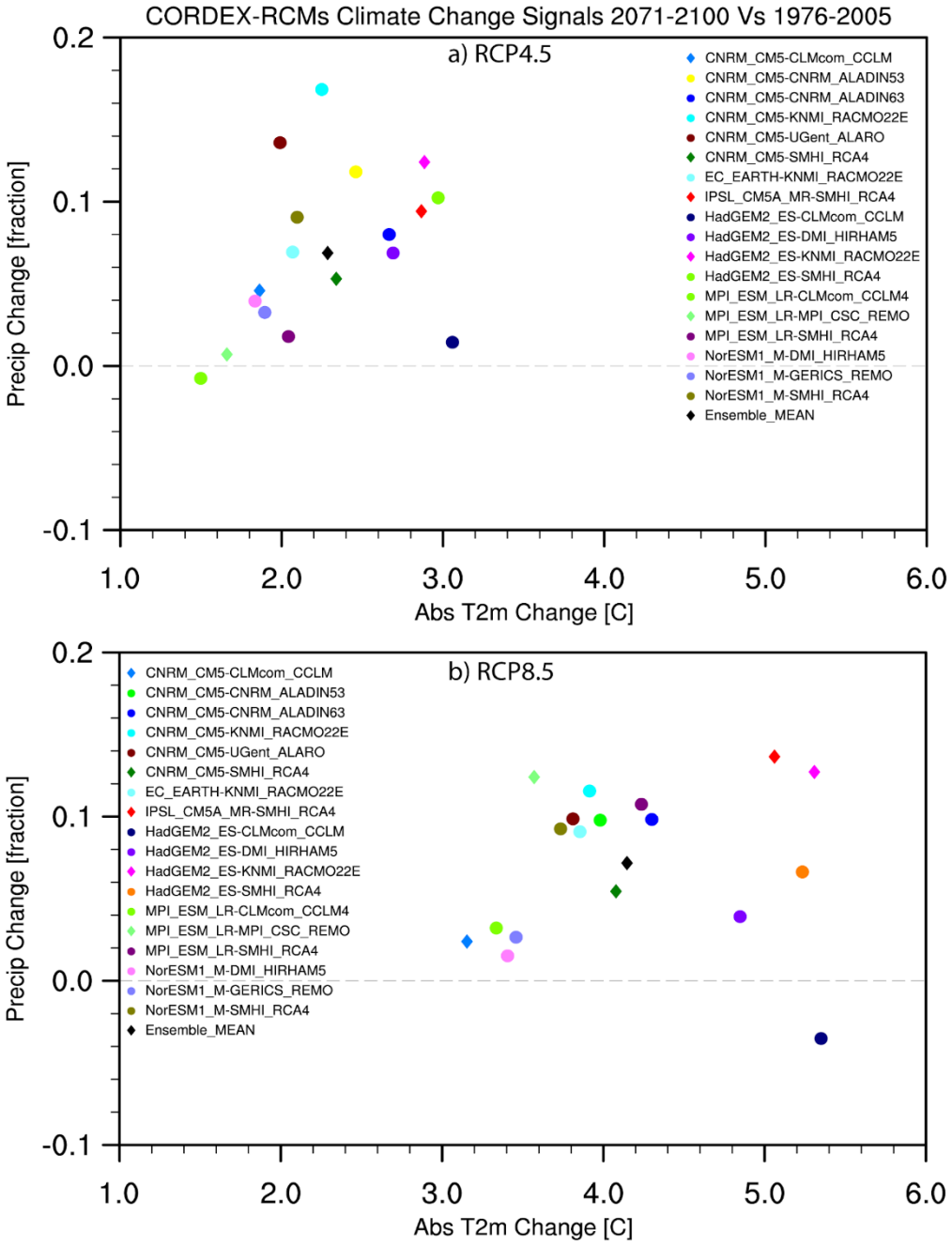

Figure 5 Change in temperature versus change in precipitation under a) RCP4.5 and b) RCP8.5 scenarios. The ensemble-mean (black diamond) and five selected models are shown with diamond shaped markers.

Table 2 List of most suitable models selected for the climate change study over the TBR MDD area.

No.	Driving Global Climate Model (GCM)	Regional Climate Model (RCM)	Abbreviation
1	CNRM-CERFACS-CNRM-CM5	CLMcom-CCLM4-8-17_v1	CNRM-CM5_CLMcom-CCLM4
2	IPSL-IPSL-CM5A-MR	SMHI-RCA4_v1	IPSL-CM5A-MR_SMHI-RCA4
3	MOHC-HadGEM2-ES	KNMI-RACMO22E_v2	HadGEM2-ES_KNMI-RACMO22E
4	MPI-M-MPI-ESM-LR	MPI-CSC-REMO2009_v1	MPI-ESM-LR_MPI-CSC
5	CNRM-CERFACS-CNRM-CM5	SMHI-RCA4_v1	CNRM-CM5_SMHI-RCA4

The selected five models presented in Table 2 and shown in Figure 5 with diamond shape markers, represent the full spectrum of future climate change by including the models covering the four extremes (wet, dry, cold and hot) and the one which is closest to the ensemble mean of all 18 models. The model CNRM-CM5_SMHI-RCA4 is closest to the ensemble mean. During the final selection process, the already excluded models (Figures 3 & 4) are not considered. Moreover, the selection is based on RCP4.5 and the same models are selected for the RCP8.5 scenario.

- **Bias-Correction of Selected Models**

Climate models generally produce biased simulations of variables such as temperature and precipitation. It is necessary to remove these biases before using the model-simulated fields in applications that have nonlinear sensitivities to biases, such as land surface or hydrological modelling. The choice of the bias correction method is particularly important in climate change impact studies since bias correction can alter model projected mean changes.

Bias correction is the process of scaling climate model outputs to account for their systematic errors, in order to improve their fitting to observations. Several bias correction methods exist. Linear scaling corrects projections based on monthly errors. Further bias correction focusing on days with precipitation can be obtained by the local intensity scaling approach. The power transformation approach can correct biases in the mean and variance. Quantile mapping can correct the distribution function of a given variable usually utilizing a gaussian or gamma distribution function to improve its fitting to observations. Most of such approaches focus on correcting precipitation and time series supplied by climate projections to improve their fitting to observations, regardless of the extreme value behaviour. Quantile mapping tries to improve the fitting of higher values of precipitation through a gamma distribution function. We have analysed several methods which include Scale Distribution Mapping (SDM) and Quantile Mapping and finally selected the most suitable methods: EDCDFm and Presrat.

The bias correction method EDCDFm (Li et al. 2010) is used for bias-adjustment of temperature and Presrat (Pierce et al. 2015) for precipitation. They are conceptually

similar techniques, although they differ in detail. Each is equivalent to simple quantile mapping over the historical era. For future periods, EDCDFm constructs the bias-corrected Cumulative Distribution Function (CDF) as the observed historical CDF plus the model-predicted future change computed at each quantile. In other words, the target CDF for the future conditions becomes the historical CDF added quantile-by-quantile to the CDF of future model changes. Presrat is similar but constructs the bias-corrected CDF as the observed historical CDF times the model-predicted factor by which values at that quantile change in the future. Presrat also multiplies by a factor calculated to ensure that the future bias-corrected change in mean value matches the original model's predicted change in mean value and applies a zero-precipitation threshold so that over the historical period, the number of zero-precipitation days in the model matches that observed.

Daily data of five selected climate models (Table 2) is first resampled to the E-OBS grid and then bias-corrected against the E-OBS gridded observation described in the previous section. In order to estimate the true added value of the application of bias correction, it is necessary to see its performance at the spatial scale. For this purpose, Figure 6 is presented to show spatial results for maximum and minimum temperature as well as precipitation. Results show a very satisfactory performance of the bias correction for all the three variables at annual scale. The temperature minimum over the Austrian Tyrol as well as maximum over Istria and north Adriatic coastal zone are well captured by the model after bias correction. Similarly, for precipitation, the maximum over the relatively wet mountainous regions in Slovenia, and the dryness in the eastern part of the domain is captured very well by the bias-corrected model. All the results presented here show a marked improvement in the results of the RCM after the application of bias correction. Based on these results, it is confidently inferred that the bias corrected dataset can now be used to force the impact models. Figure 6 also shows the historical climatological mean values of temperature and precipitation for the reference period 1976-2005. This information is used further in the results section while interpreting the changes in extremes. The proceeding sections contain information on the climate change signals and extreme events obtained from these bias-corrected RCMs.

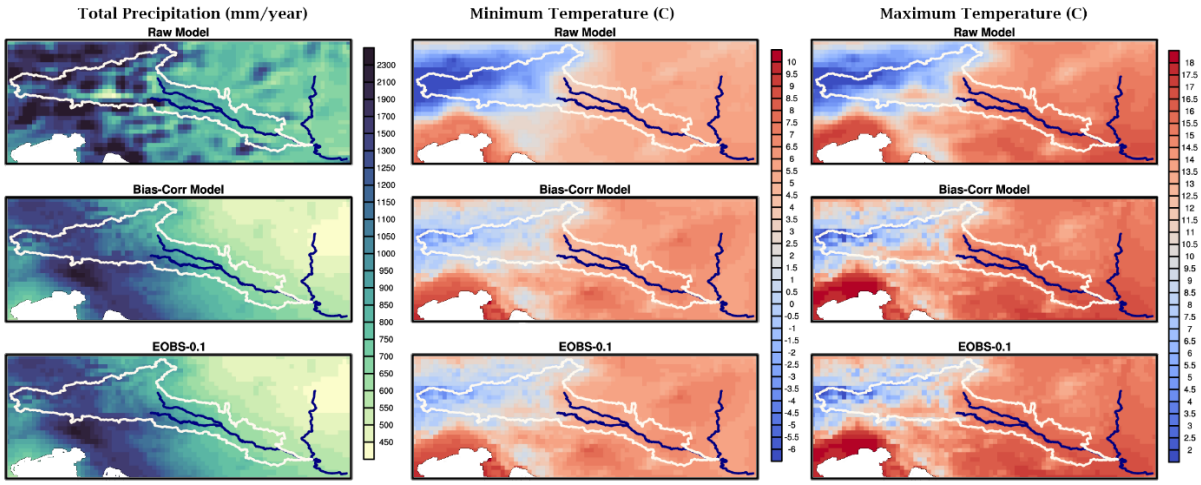

Figure 6 Validation of Bias-correction for mean model CNRM-CM5_SMHI-RCA4. The first row shows the 30-year mean of annual precipitation, minimum temperature and maximum temperature for the historical period 1976-2005. The second and third rows show the same variables from bias-corrected model and observations (E-OBS-0.1), respectively.

- ## Climate Extreme Indices

The present section deals with the changes in extreme climatic events associated with changes in the mean climate and climate variability. An extreme event is generally defined as the occurrence of a value of a climate variable above (or below) a threshold value near the upper (or lower) ends ('tails') of the range of historical values (or control period) of the variable. Some climate extremes (e.g., droughts, floods) may be the result of an accumulation of weather or climate events that are, individually, not extreme themselves (though their accumulation is extreme). Also, weather or climate events, even if not extreme in a statistical sense, can still lead to extreme conditions or impacts, either by crossing a critical threshold in a social, ecological, or physical system, or by occurring simultaneously with other events. Based on the multi-model ensemble of the selected regional climate models, we calculate temperature related extreme events (heat waves, summer days, tropical nights, cold waves, frost and ice days). Moreover, precipitation-related extreme climate events that are relevant for hydrology and water resources, forestry and biodiversity are also calculated. The full list of selected extreme events along with descriptions and units is given in Table 3. All the definitions of extremes are taken from the indices defined by the joint CCl/CLIVAR/JCOMM Expert Team on Climate Change Detection and Indices (ETCCDI).

Table 3 List of temperature and precipitation-based extreme indices along with definitions and units used in this study

ID.	Indicator Name	Indicator Description	Units
FD0	Frost days	Annual count when daily minimum temperature < 0°C	days
SU25	Summer days	Annual count when daily max temperature > 25°C	days
TR20	Tropical nights	Annual count when daily min temperature > 20°C	days
ICD0	Ice Days	Annual count when daily max temperature < 0°C	days

HWDI	Heat wave duration index	No. days in intervals of at least 6 days with Tmax > 5°C+mean calculated for each calendar day (based on reference period) using running 5-day window	days
HWFI	Warm spell days	No. of days in intervals of least 6 days with Tmean > 90th percentile calculated for each calendar day (based on reference period) using running 5-day window	days
CWDI	Cold wave duration index	See HWDI, but Tmin < mean-5°C	days
CDFI	Cold spell days	See HWFI, but Tmean < 10th percentile	days
CDD	Consecutive dry days	Maximum number of consecutive dry days (annual) when PR < 1.0 mm, also referred to as 'longest dry spell' (annual)	days
CWD	Consecutive wet days	Maximum number of consecutive days when precipitation >= 1.0 mm (annual)	days
RX1day	Max 1-day precipitation amount	Annual maximum 1-day precipitation	mm
RX5day	Max 5-day precipitation amount	Annual maximum consecutive 5-day precipitation	mm
SDII	Simple daily intensity index	The ratio of annual total precipitation to the number of wet days (= 1 mm)	mm/d
R95p	Very wet days	Annual total precipitation from days > 95th percentile	mm
R99p	Extremely wet days	Annual total precipitation from days > 99th percentile	mm
PRCPTOT	Annual total wet-day precip	Annual total precipitation from days = 1mm	mm
R10	Number of heavy rain days	Annual count of days when PR ≥ 10 mm	days
R20	Number of very heavy rain days	Annual count of days when PR ≥ 20 mm	days

III. Results

- ## Climate Change Impact Assessment on Seasonal & Annual Basis

Temperature

This section presents the results of mean changes in the variables of temperature while the next section describes the results for precipitation. All the figures showing time series (line plots) and the box-and-whisker plots are based on mean values of the boxed region highlighted in Figure 2. The annual and seasonal anomalies of mean temperature from the base period 1976-2005 are presented in Figures 7 and 8. The similar plots for minimum and maximum temperature are given in Appendix A. The Figures 7 and 8 show anomalies in daily mean temperature for four seasons, winter and summer half years and

annual basis under two different scenarios. Although there is year to year variation among the five models, all the models are consistent in predicting the warming trend in all seasons. The warming trend levels off in the second half of the century under RCP4.5 but continues to increase under RCP8.5. The warming becomes two-fold by the end of the century under stronger climate change RCP8.5 scenario than under RCP4.5. The spread among the models is more in winter as compared to summer. The average Dec–Jan–Feb (DJF) temperature increases up to 2.2 °C till 2100 under RCP4.5 and around 4.2°C under RCP8.5. This can have huge implications in areas with snow cover. Such an increase in mean temperature (and minimum temperature, see Appendix A) will reduce the availability of snow in winter and can trigger early snowmelt in spring resulting in significant changes in the hydrological cycle of the area.

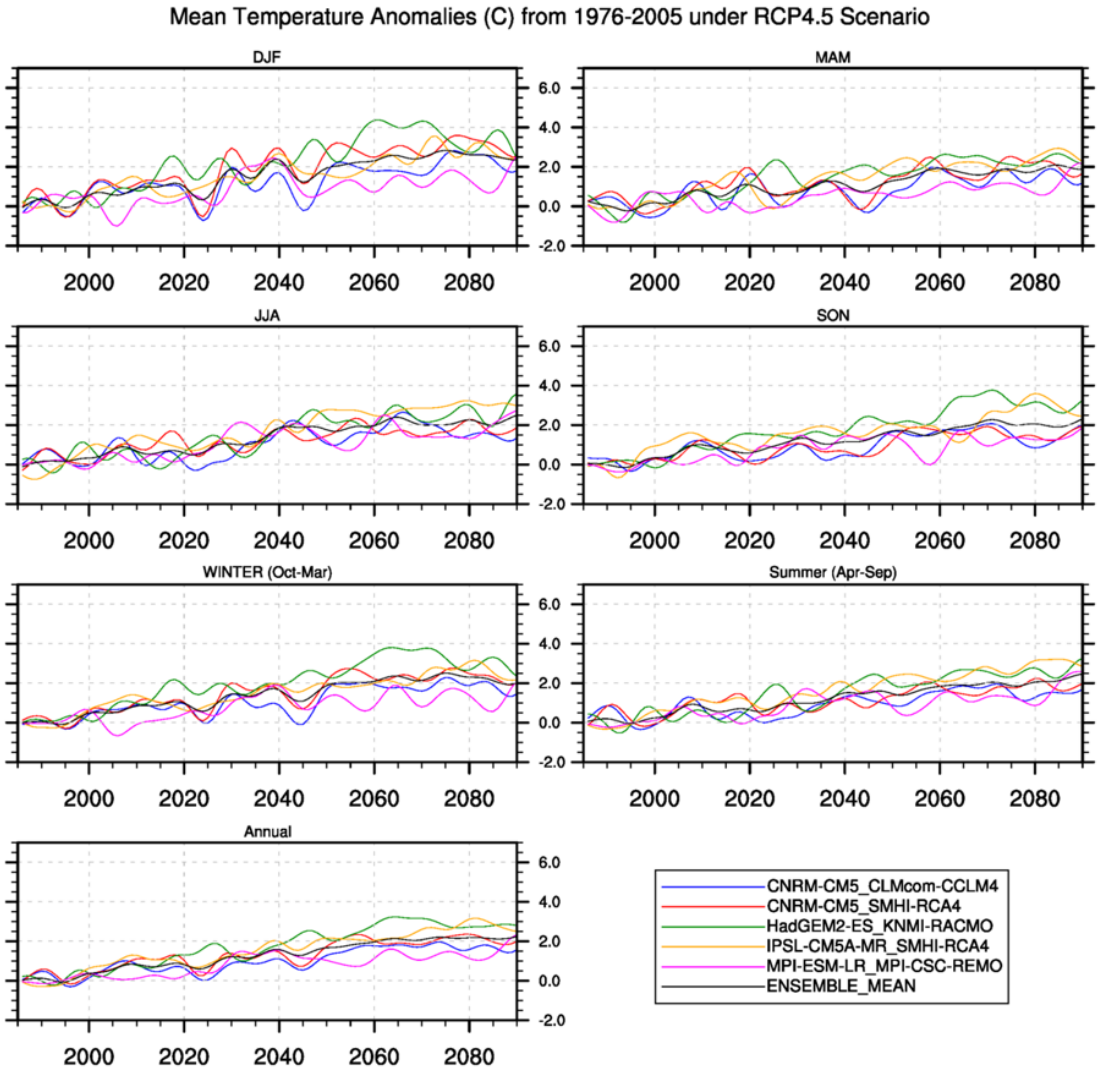

Figure 7 Average annual and seasonal anomalies of daily mean temperature (in °C) from the base period 1976-2005 under RCP4.5 for the area highlighted with rectangle in figure 2

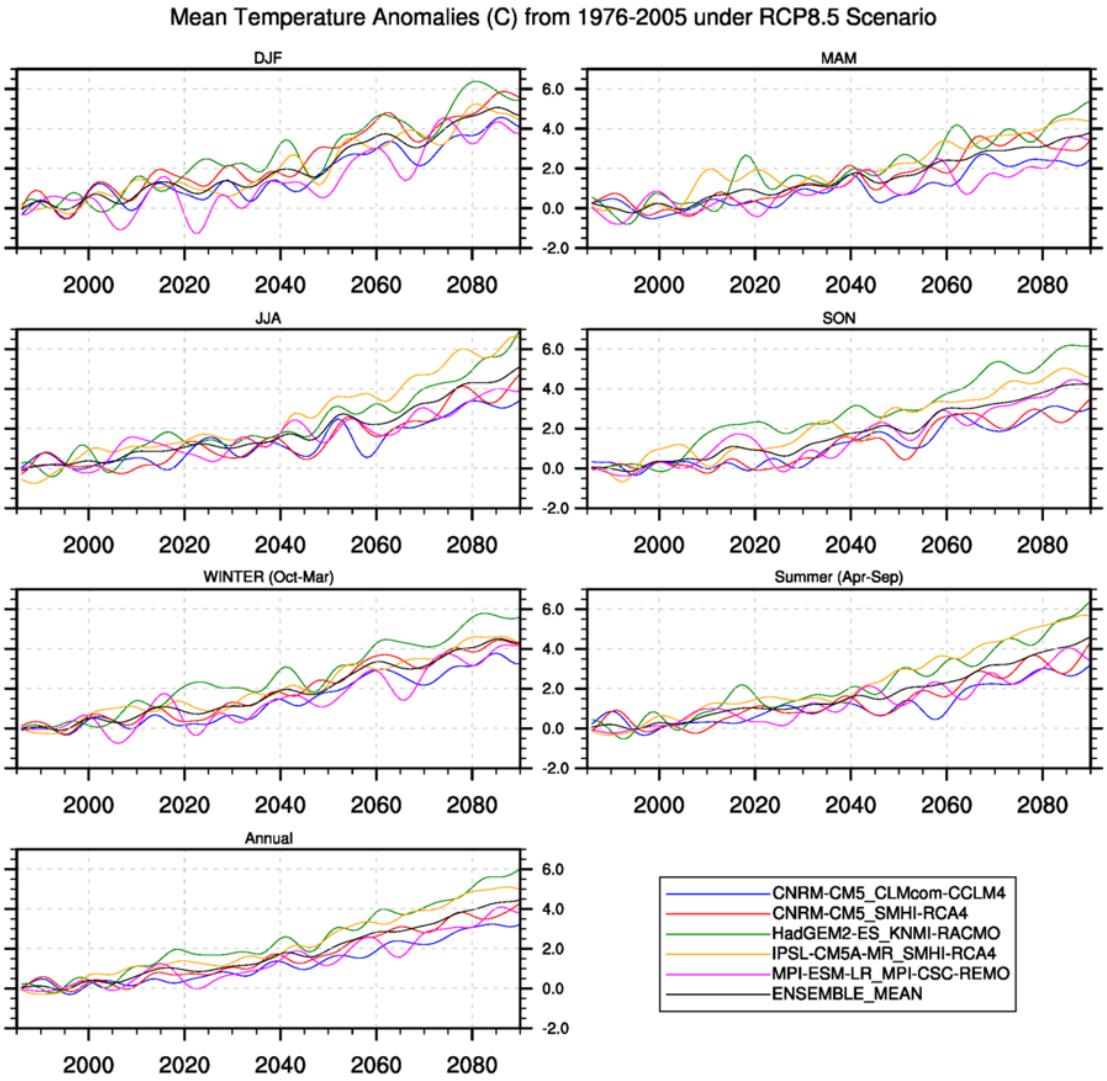

Figure 8 Average annual and seasonal anomalies of daily mean temperature (in °C) from the base period 1976-2005 under RCP8.5 for the area highlighted with rectangle in Figure 2

Figure 9 shows seasonal and annual changes in mean temperature based on ensemble mean of the five models for the time-slices 2021-2050 (near future), 2036-2065 (mid-century) and 2071-2100 (end-century) as compared to reference period 1976-2005. The box plot is based on median, 25th and 75th percentiles of precipitation anomalies for a given time while the whiskers represent the minimum and maximum within the period. The stabilization scenario RCP4.5 is characterized by gradual increase in temperature through the century in all seasons while more abrupt and drastic changes in temperature are evident under RCP8.5 during the second half of the century. The changes are stronger in winter and fall as compared to spring and summer.

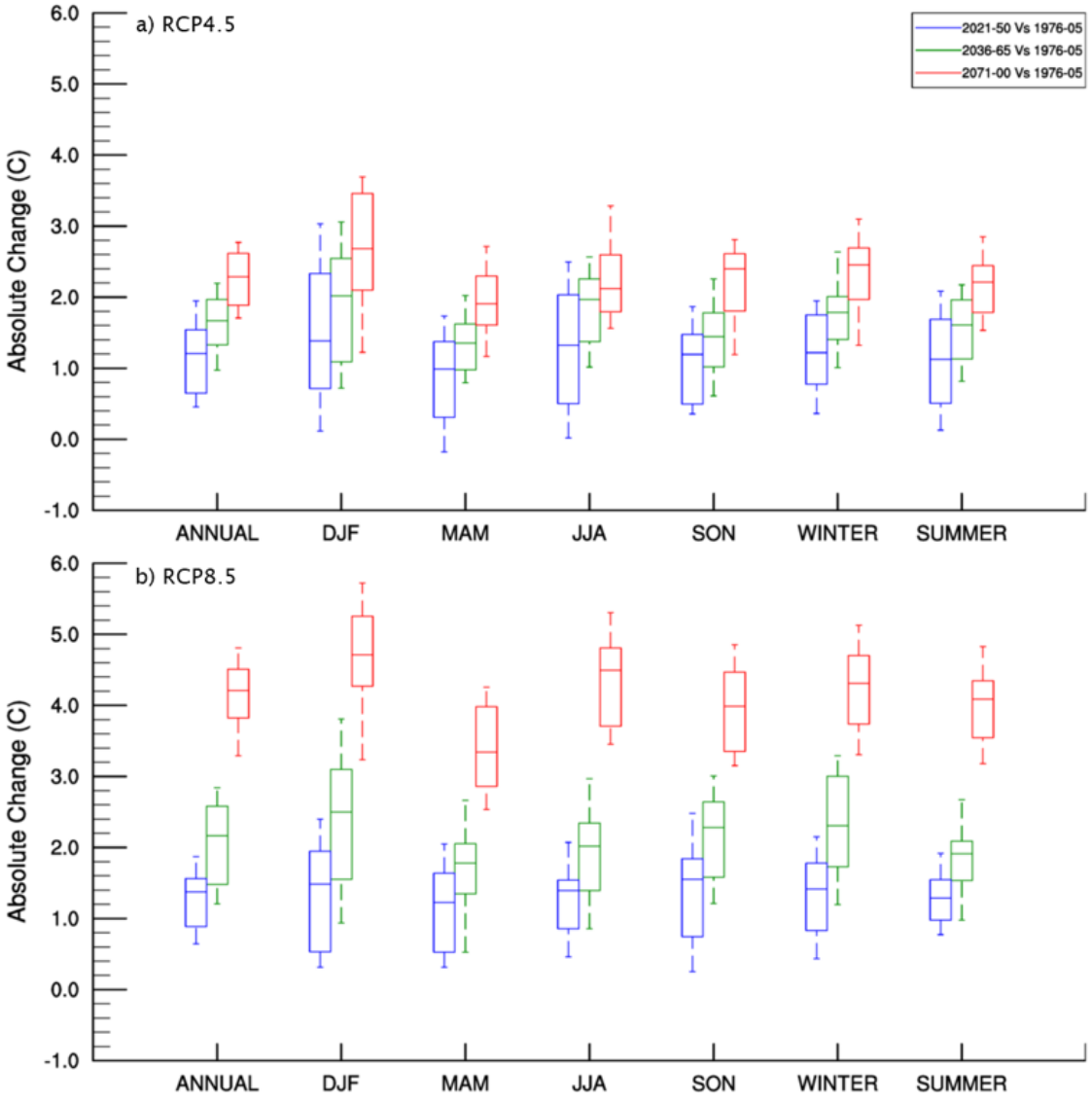

Figure 9 Box and whisker plot showing ensemble-based absolute changes in annual and seasonal temperature (in °C) for 2021-2050, 2036-2065 and 2071-2100 from the base period 1976-2005 under two different scenarios RCP4.5 (above) and RCP8.5 (below).

To estimate the impact of temperature change on local ecosystems and biodiversity, it is necessary to see the climate change signals at spatial scale. Figures 10 and 11 show the spatial distribution of change in temperature for different future periods for Dec–Jan–Feb (DJF) and Jun-Jul-Aug (JJA) respectively. The figures show uniform increase of temperature over the whole domain under both RCPs. The warming is stronger in winter months as compared to summer.

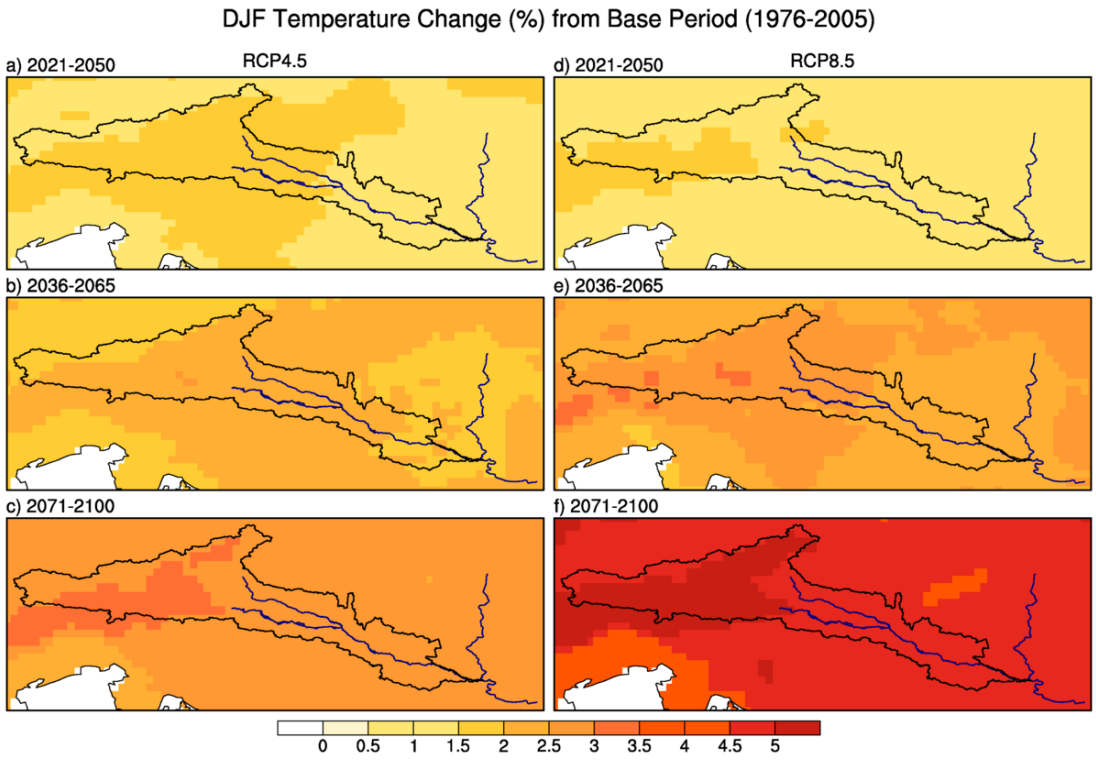

Figure 10 Spatial distribution of DJF temperature changes (in °C) from reference period 1976-2005 based on ensemble-mean of five selected models for different future periods (rows) under two emission scenarios (columns).

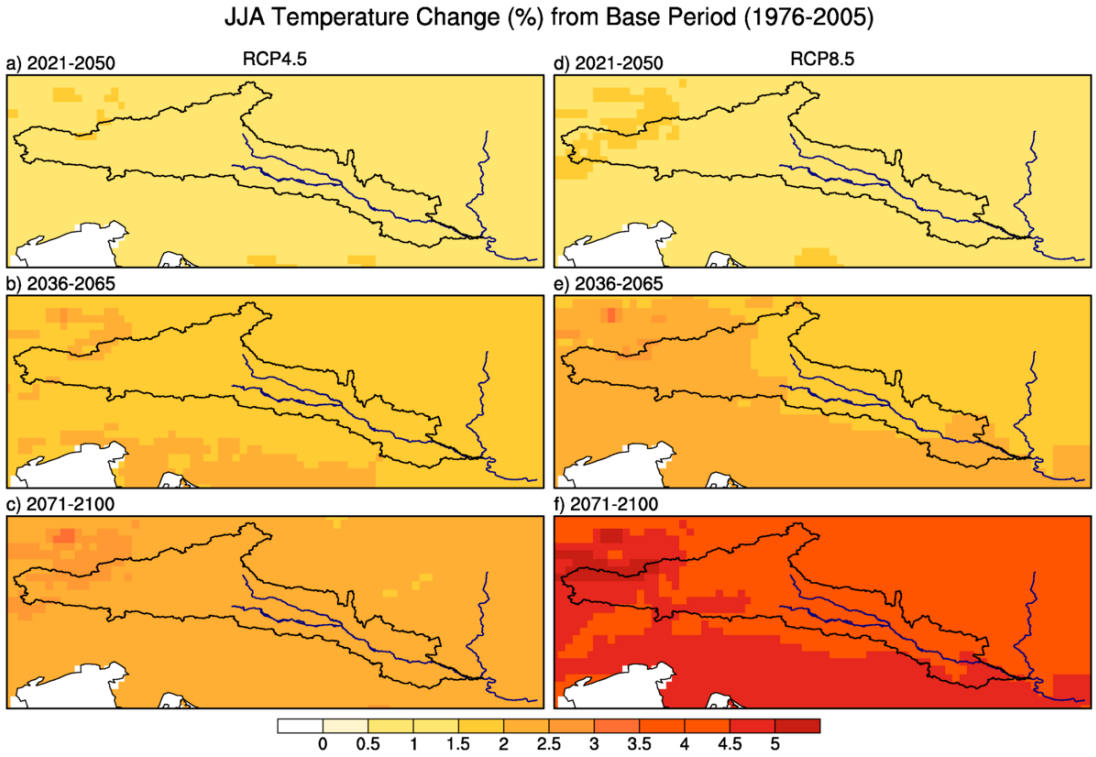

Figure 11 Same as Figure 10 but for JJA

Precipitation

Precipitation is one of the most important meteorological parameters, as changes in precipitation pattern directly impact the hydrological regime of the river basins in the area under investigation. Contrary to temperature, Figures 12 and 13 show strong year to year variations in precipitation change. The magnitude of change is quite different among the models but there are clear trends of significant increase in winter precipitation whereas a slight reduction of summer precipitation can be determined. The magnitude of increase of winter precipitation is about 15% (ensemble mean) under RCP4.5 while the high emission scenario RCP8.5 will lead to an increase of about 20% by the end of the century.

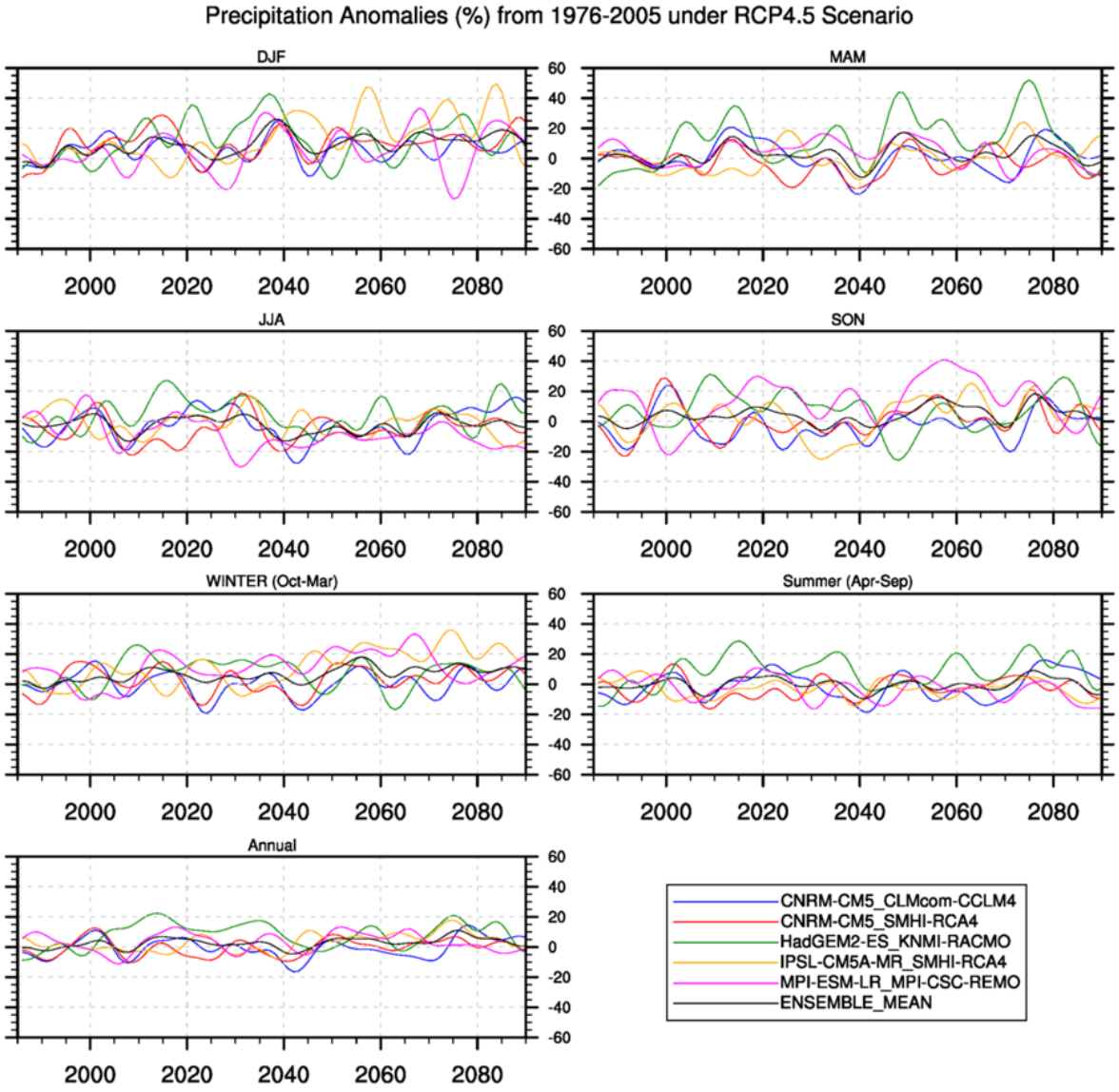

Figure 12 Average annual and seasonal anomalies of daily precipitation (in %) from the base period 1976-2005 under RCP4.5 for the area highlighted with rectangle in Figure 2

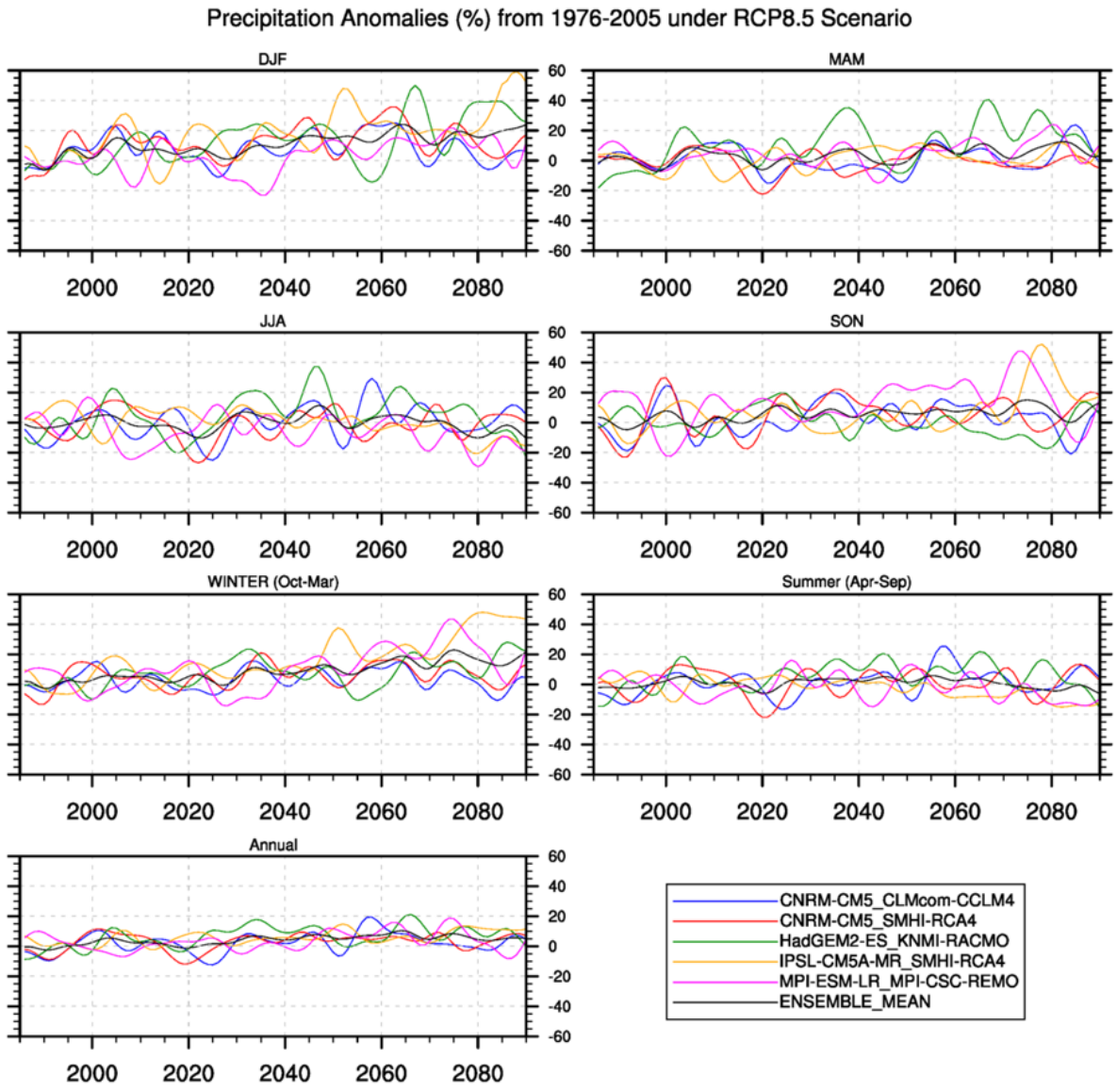

Figure 13 Average annual and seasonal anomalies of daily precipitation (in %) from the base period 1976-2005 under RCP8.5 for the area highlighted with rectangle in Figure 2

Figure 14 depicts an even more clear picture of seasonal changes in precipitation on different timescales under both RCPs. The box and whisker plot based on the ensemble mean of five models shows the redistribution of precipitation among the season resulting in overall less change (max. 10% increase) on annual scale but significant increase in precipitation in DJF and SON, especially in mid-century and end-century. The reduction in JJA precipitation is strongest in the second half of the century in the RCP8.5 scenario.

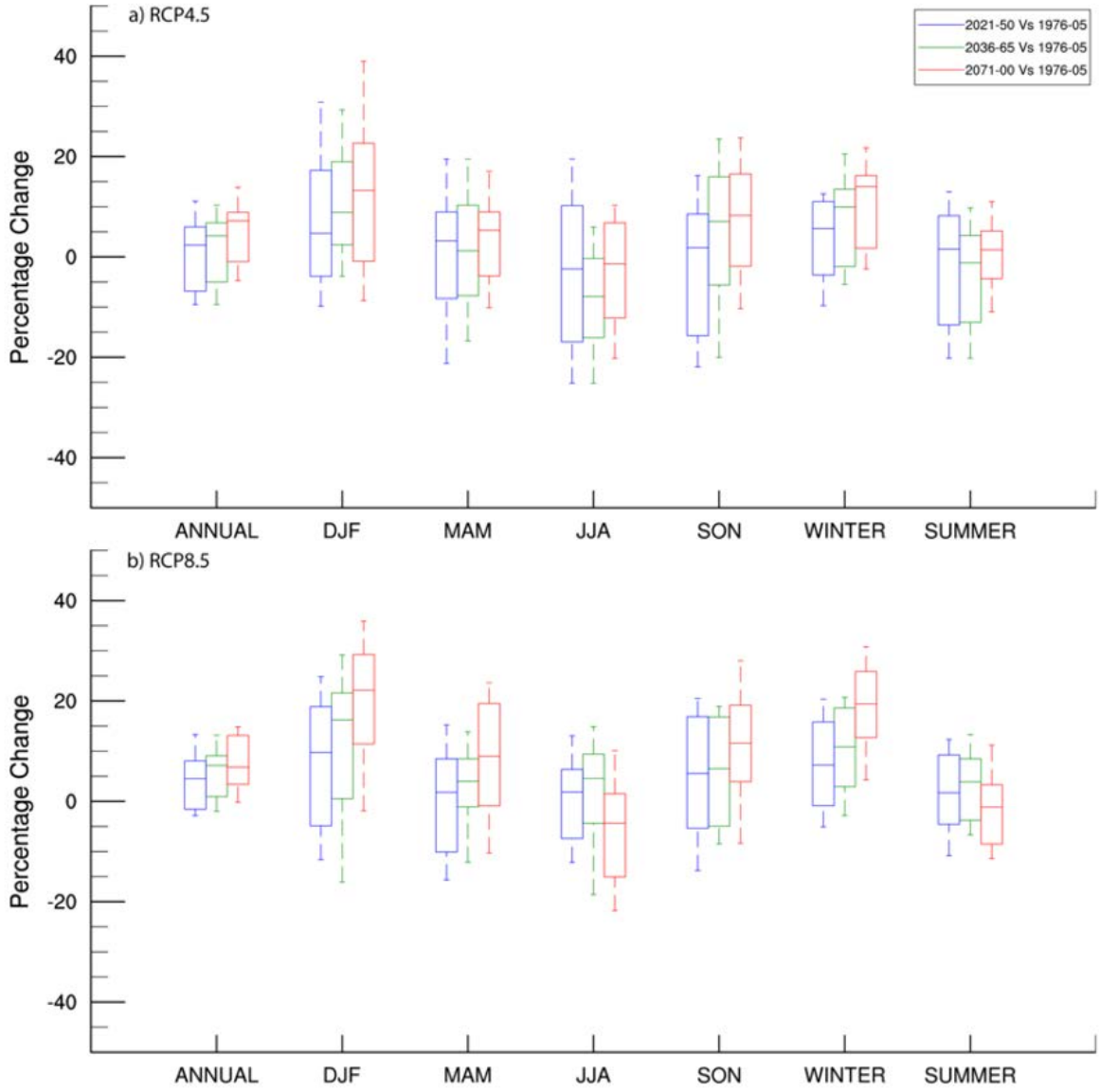

Figure 14 Box and Whisker plot showing ensemble-based relative changes in annual and seasonal precipitation (in %) for 2021-2050, 2036-2065 and 2071-2100 from the base period 1976-2005 under two different scenarios RCP4.5 (above) and RCP8.5 (below).

As the spatial distribution of precipitation is very important for the hydrological cycle, the spatial patterns of precipitation changes are analyzed in Figures 15 and 16. The spatial plots show the gradual increase of winter precipitation towards the end of the century. These changes are more prominent under high emission scenario RCP8.5. Interestingly, most of the increase is centered over the Great Hungarian Plains. Figure 16 shows a decrease in summer precipitation over some parts of Slovenia and Croatia while the rest of the regions experience only minor changes (-5% to 5%).

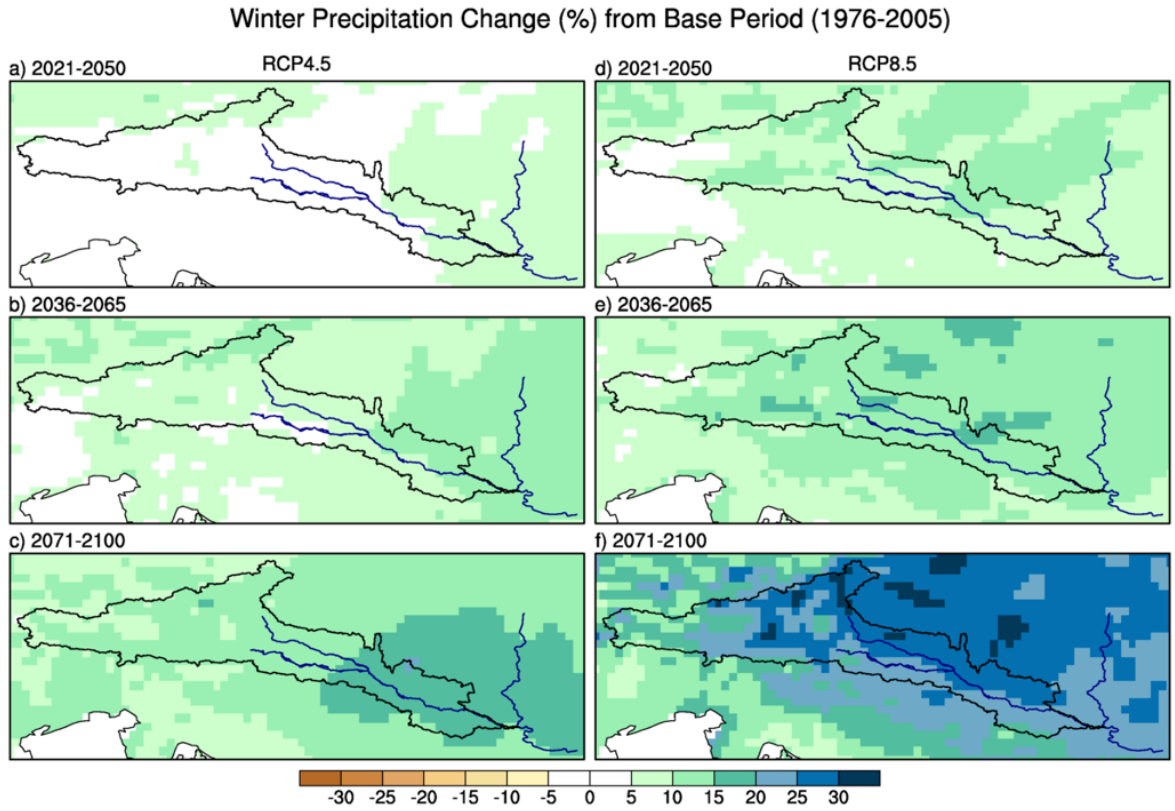

Figure 15 Spatial distribution of winter precipitation changes (in %) from reference period 1976-2005 based on ensemble-mean of five selected models for different future periods (rows) under two emission scenarios (columns)

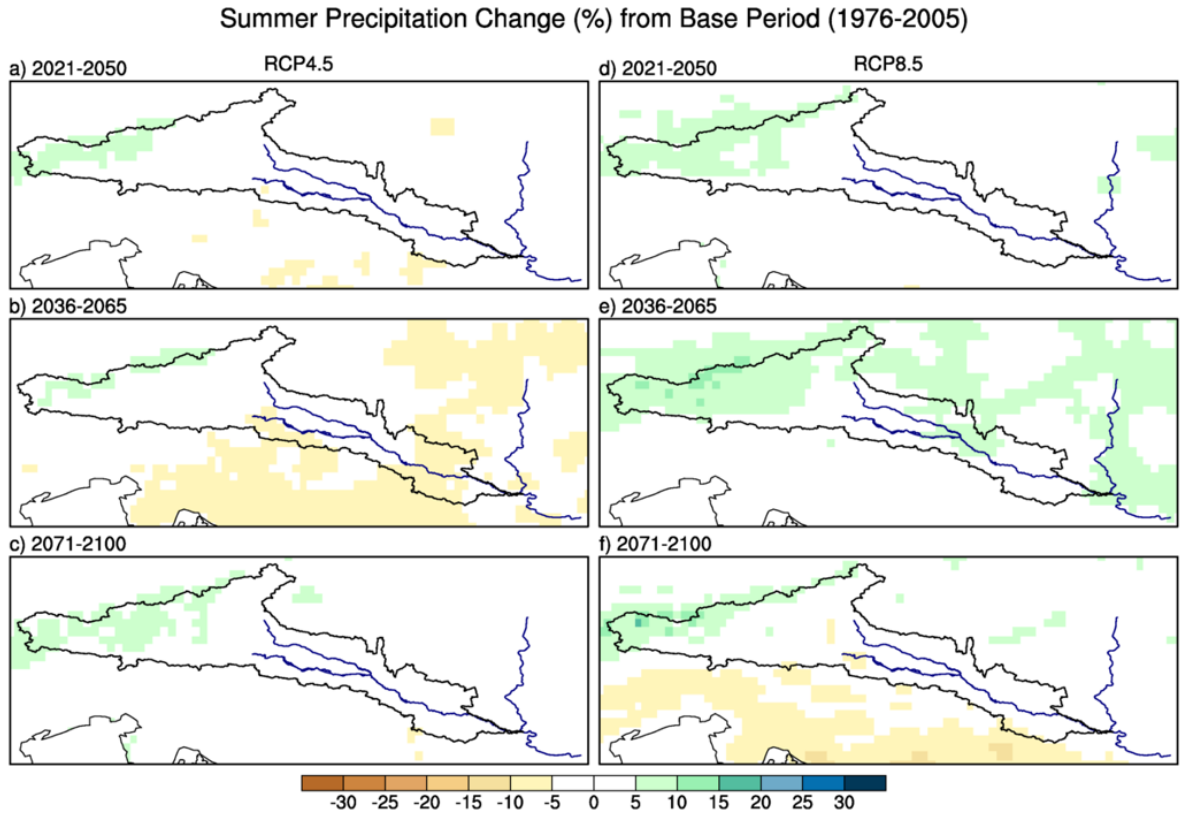

Figure 16 Same as Figure 15 but for summer

Results of the changes in temperature and precipitation clearly point towards a hotter and wetter climate especially in winter under future warming. However, it will be interesting to find out how these changes manifest themselves in the form of climatic extremes which are explored in the proceeding section.

- **Climate Extreme Indices Assessment and Impacts**

While the main focus of the previous sections was climate change signals of temperature and precipitation, the present section deals with changes in extreme climatic events associated with changes in the mean climate and climate variability. The variability and change in the patterns of climatic extremes are shown in spatial plots in this section. All figures displaying extreme indices are based on the ensemble-mean of indicators calculated from individual models. The figures also show minimum, maximum and mean value for the reference period (below the coloured bars). For brevity, some of the variables are presented in the main text, while some of the variables are included in Appendix B.

Figure 17 presents an important indicator for dryness i.e., consecutive dry days (CDD). It is calculated by counting the maximum number of consecutive dry days within a year when precipitation is less than 1mm/day, also referred to as the 'longest dry spell'. While complementing most of the previously shown figures for precipitation changes, this Figure points towards the wetting signals over the TBR MDD region by showing a reduction of consecutive dry days in the future decades. This pattern is more obvious in the mid and end century, while the near-future shows some increase in CDD over a few regions as seen in panel (a) and (d).

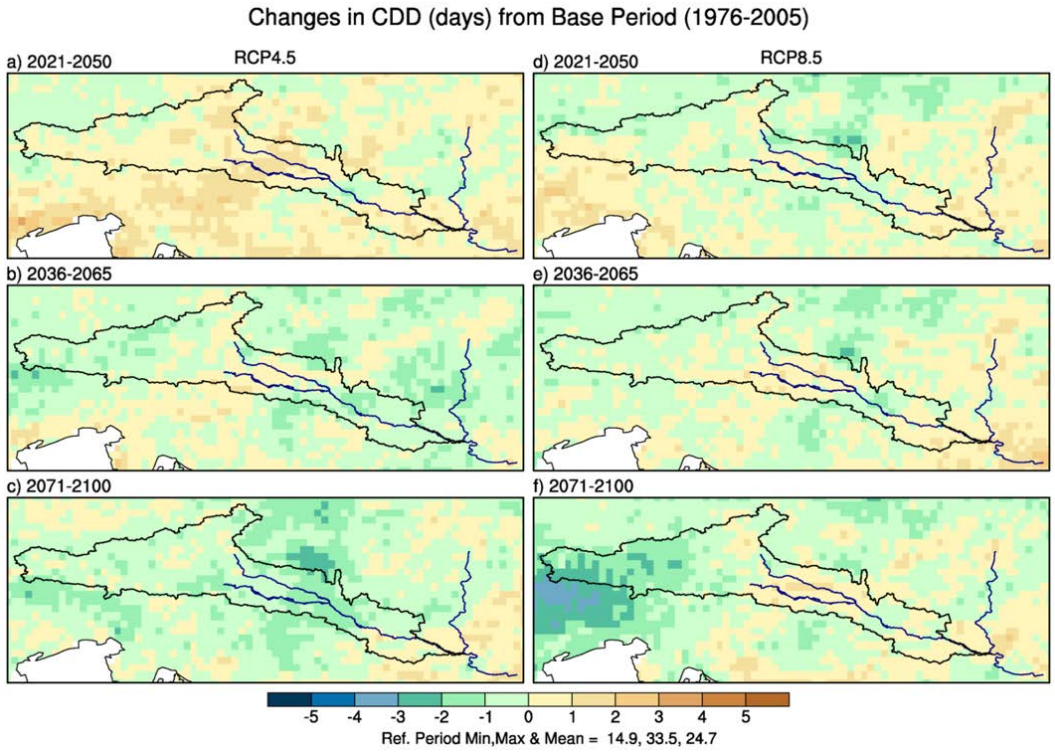

Figure 17 Differences in the number of consecutive dry days (annual) using an ensemble mean of five selected models. The differences are determined through calculating the means of each time-period and comparing them with the means of the reference period (1976-2005).

A similar figure of consecutive wet days (CWD), which is the count of the maximum number of consecutive wet days (annual) when precipitation is greater than 1mm/day, is shown in Appendix B. Figure 18 shows changes in summer days which is the annual count of days when daily maximum temperature is greater than 25°C. Under both scenarios, all future time periods show increasing trends in summer days. The trend is stronger in hotter regions (See Figure 6 for spatial distribution of maximum temperature) which means the hotter periods will last even longer in future in these regions. During the reference period, a maximum of 102 summer days per year are counted, and this number will increase by 30-50 days under RCP4.5 and 40-60 days under RCP8.5 in the later half of the century. Increase in summer days also means longer vegetation periods and a significant increase in water demand for agriculture and forestry. A similar figure for tropical nights (TR20) is given in Appendix B. The tropical night index is the count of the days when the minimum temperature stays above 20°C. Increase in tropical nights can lead to a rise of mortality as it makes it difficult for the human body to stay cool especially for sick and elderly people.

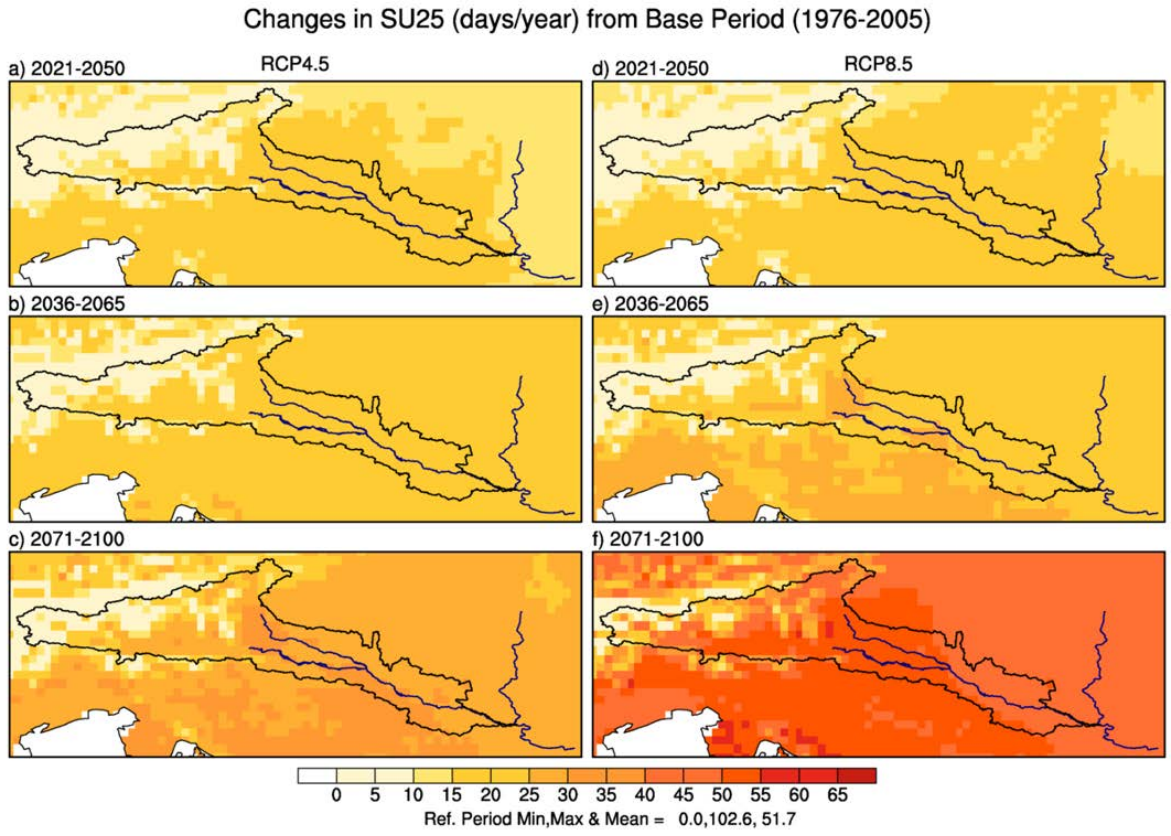

Figure 18 Differences in the number of summer days (SU25; Tmax > 25°C) using an ensemble mean of five selected models. The differences are determined through calculating the means of each time-period and comparing them with the mean of the reference period (1976-2005)

Another useful indicator relevant for water supply, tourism, human health, and the economy, is frost days (FD0). The frost days, when minimum temperatures dip below freezing are shown in Figure 19 while the ice days, when maximum temperatures never

rise above freezing point are presented in Appendix B. The decrease in the number of frost days across the TBR MDD is projected to continue throughout the 21st century, and the number is expected to decline by about half by the end of the 21st century under the high-emissions scenario RCP8.5.

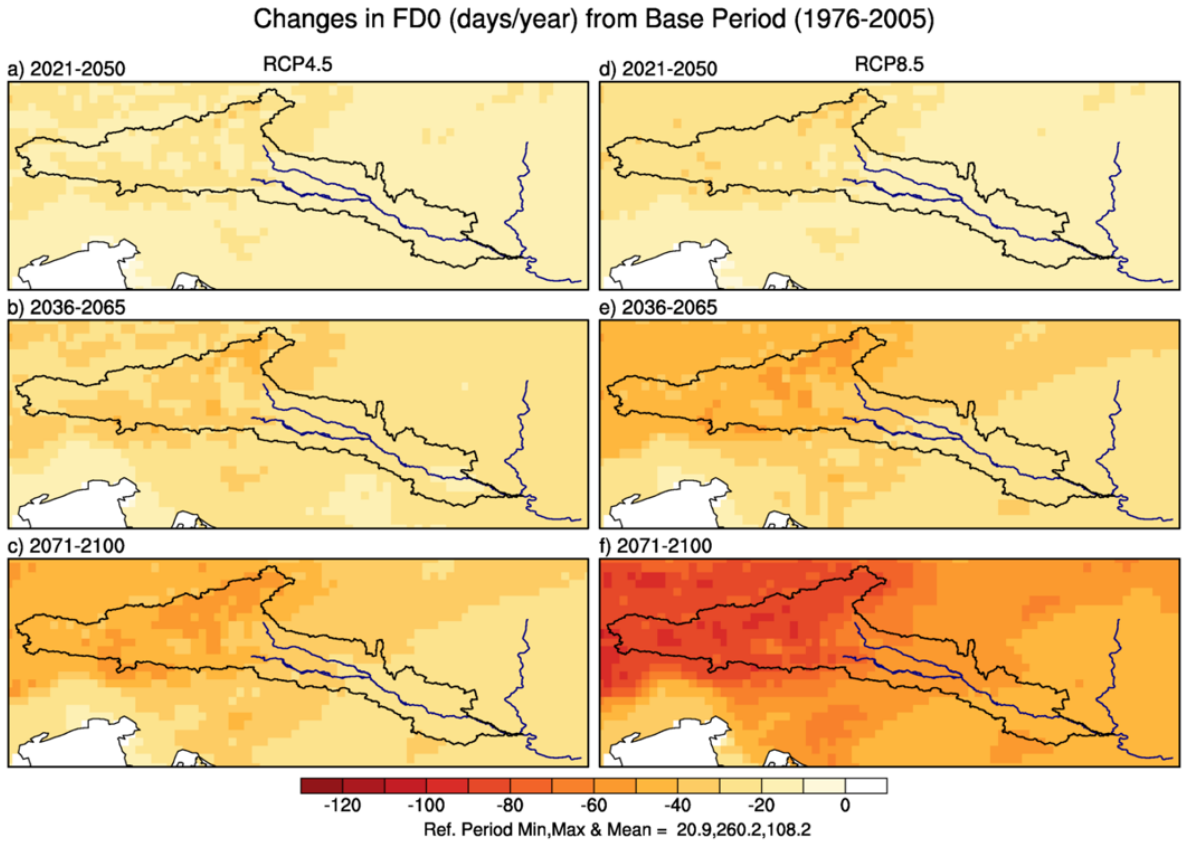

Figure 19 Differences in the number of frost days (FD0; Tmin < 0.0°C) using an ensemble mean of five selected models. The differences are determined through calculating the means of each time-period and comparing them with the mean of the reference period (1976-2005)

Despite a general decrease in frost days in future periods, an earlier start of the growing season could increase the risk of frost damage.

Figures 20 and 21 illustrate the changes in heat wave duration index (HWDI) and cold wave duration index (CWDI) respectively for the future periods under RCP4.5 and RCP8.5, with respect to the reference period 1976-2005. The HWDI is of great importance because it is a major cause of weather-related mortality. The opposite signs in the trends of CWDI and HWDI depict relative warming in the region; negative trends in CWDI and positive in HWDI predict more intense and longer heat waves in future time periods. Similarly, cold waves are observed to be shorter in changing climate throughout the 21st century. Related indices HWFI and CWFI (see Table 3) are presented in the Appendix B. Similar warming trends are observed in these extreme indices.

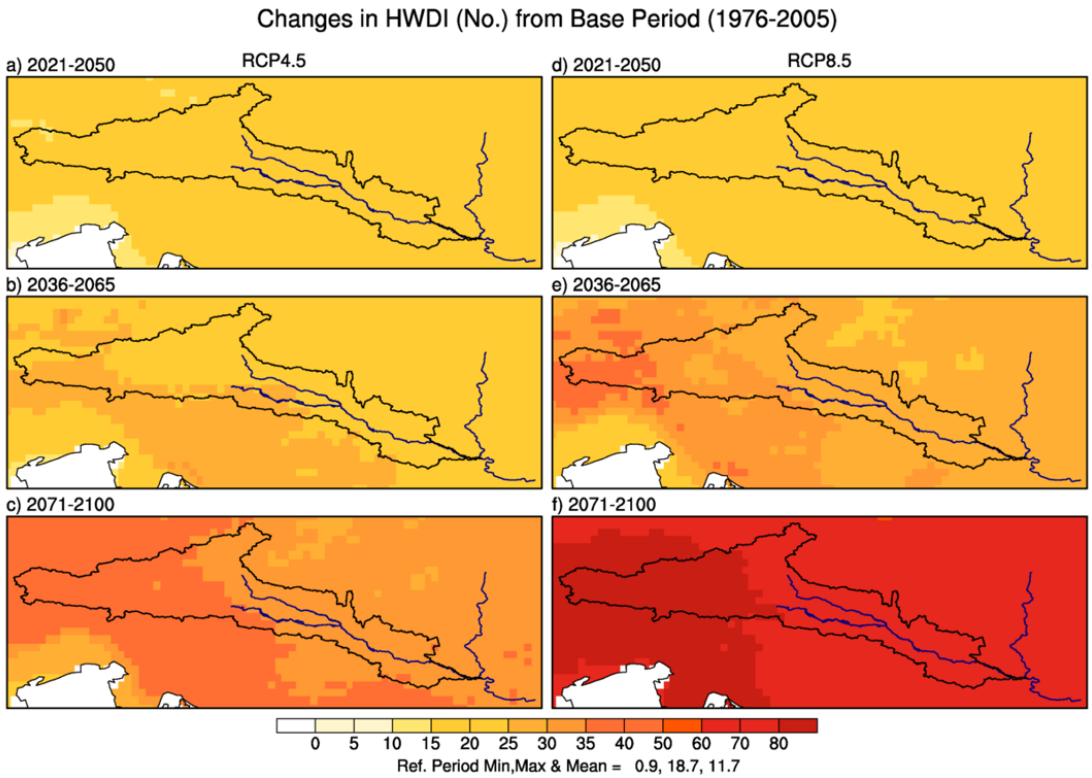

Figure 20 Differences in the heat wave duration index (HWDI; see Table 3) using an ensemble mean of five selected models. The differences determined through calculating the means of each time-period and comparing them with the mean of the reference period (1976-2005)

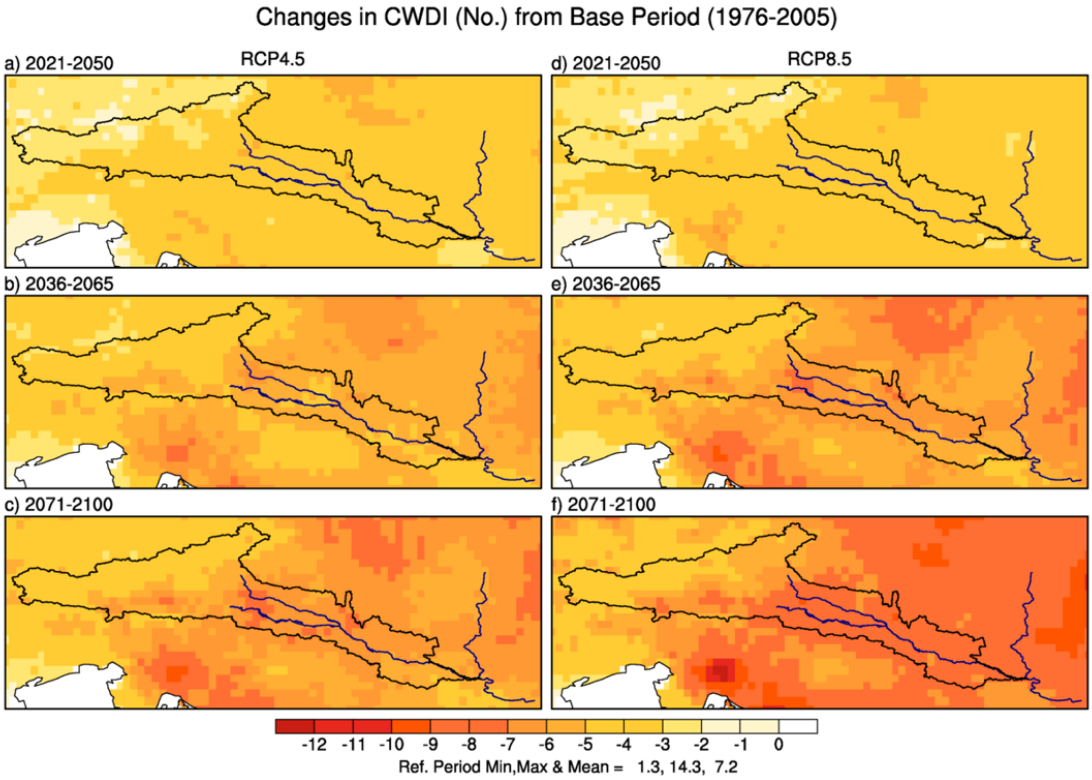

Figure 21 Differences in the cold wave duration index (CWDI; see Table 3) using an ensemble mean of five selected models. The differences are determined through calculating the means of each time-period and comparing them with the mean of the reference period (1976-2005)

Extreme precipitation plays a major role in many catastrophes at national level and can have huge implications on both the human and natural systems, mainly through flooding events. The two common extreme precipitation indices R10 (heavy precipitation days) and R20 (very heavy precipitation days) were thus calculated and changes in these indicators for future periods against the historical period are presented. Figure 22 presents future changes in R20, while trends in R10 are given in Appendix B. Both indicators consistently predict an increase in heavy precipitation days in most of the region with the highest increase seen in Austrian Tyrol. A slightly negative trend mainly in R10 is observed in the north Adriatic coastal zone.

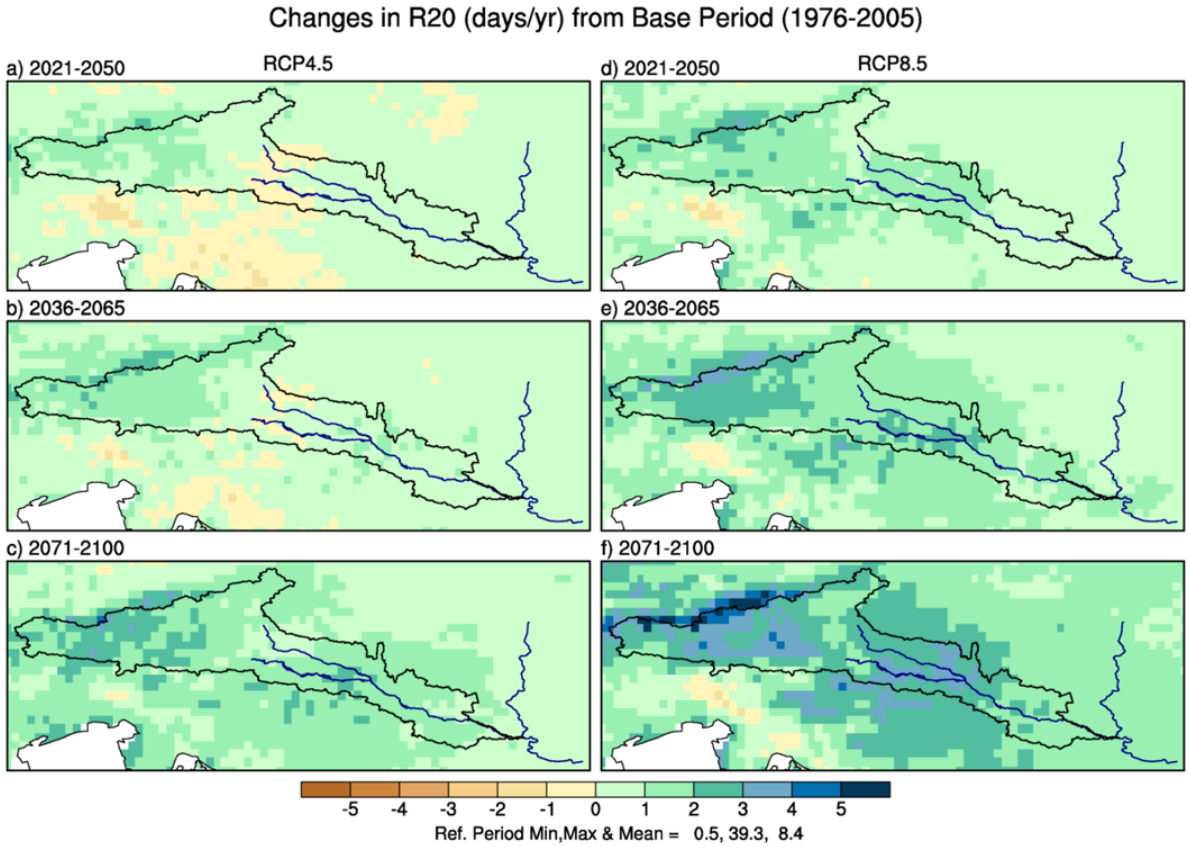

Figure 22 Differences in number of heavy precipitation days i.e., greater than 20mm symbolized by R20, using an ensemble mean of five selected models. The differences are determined through calculating the means of each time-period and comparing them with the mean of the reference period (1976-2005).

Changes in the magnitude of extreme precipitation are also calculated which is shown in Figures 23 and 24. The indicators R95p (very wet days) and R99p (extremely wet days) represent the changes in annual total precipitation from days greater than 95th percentile and 99th percentile respectively between the historical period (1976-2005) and three future periods up to 2100. Just like shown by R10 and R20, an increase in extreme wet days can be witnessed over almost the whole TBR MDD region except in a few regions where negative change is observed only in the near future time period under RCP4.5. Such an increase in frequency and intensity of extreme precipitation events is alarming as they are usually followed by heavy flooding events. The same increase is also reflected in Rx5day, which measures the maximum of five days of precipitation. This

climate index also measures heavy precipitation with high values corresponding to higher probability of flooding.

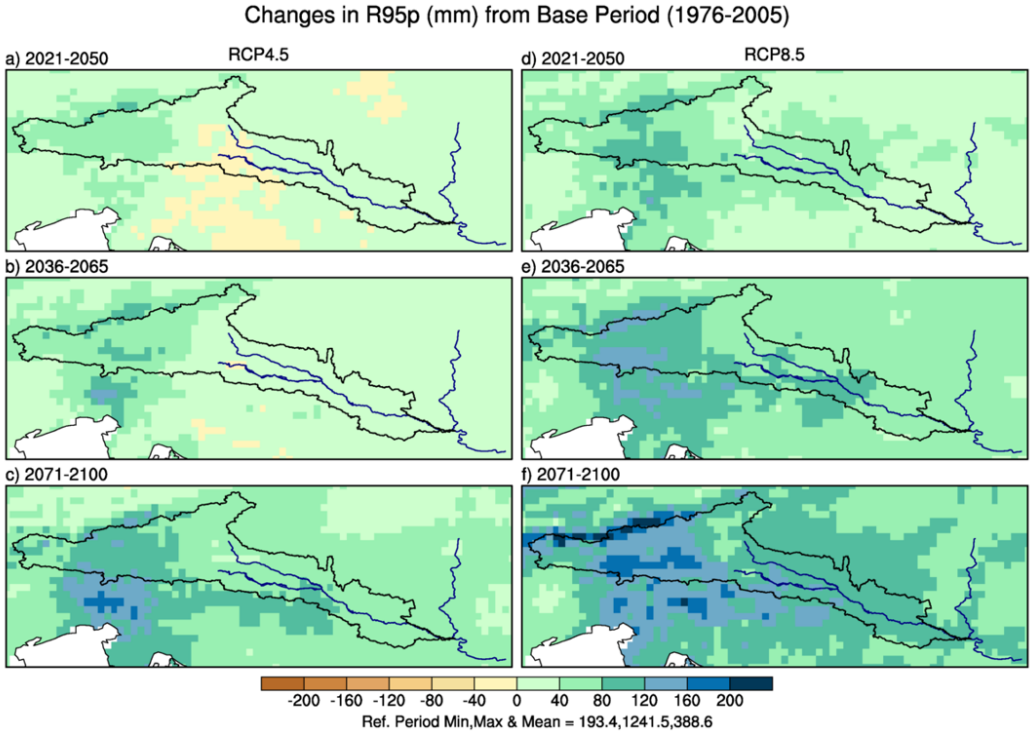

Figure 23 Differences in annual sum of very wet days R95p (See Table 3) using an ensemble mean of five selected models. The differences are determined through calculating the means of each time-period and comparing them with the mean of the reference period (1976-2005)

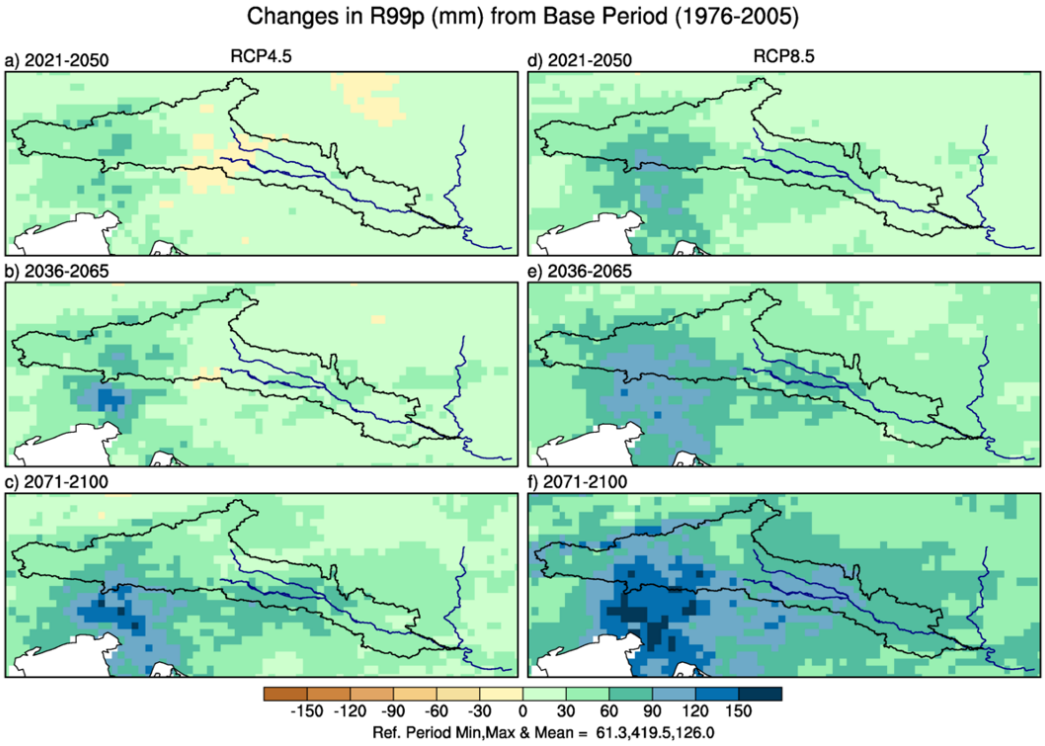

Figure 24 Differences in annual sum of extremely wet days R99p (See Table 3) using an ensemble mean of five selected models. The differences are determined through calculating the means of each time-period and comparing them with the mean of the reference period (1976-2005)

To complement the figures above, we have also plotted a simple daily intensity index (SDII) in Figure 25 which is the simple daily intensity index defined as the ratio of annual total precipitation to the number of wet days. The number of wet days is defined as the days above a threshold of 1mm. Similar to the previous figures, a gradual increase in the ratio is seen which once again points towards an increase in precipitation in the TBR MDD region.

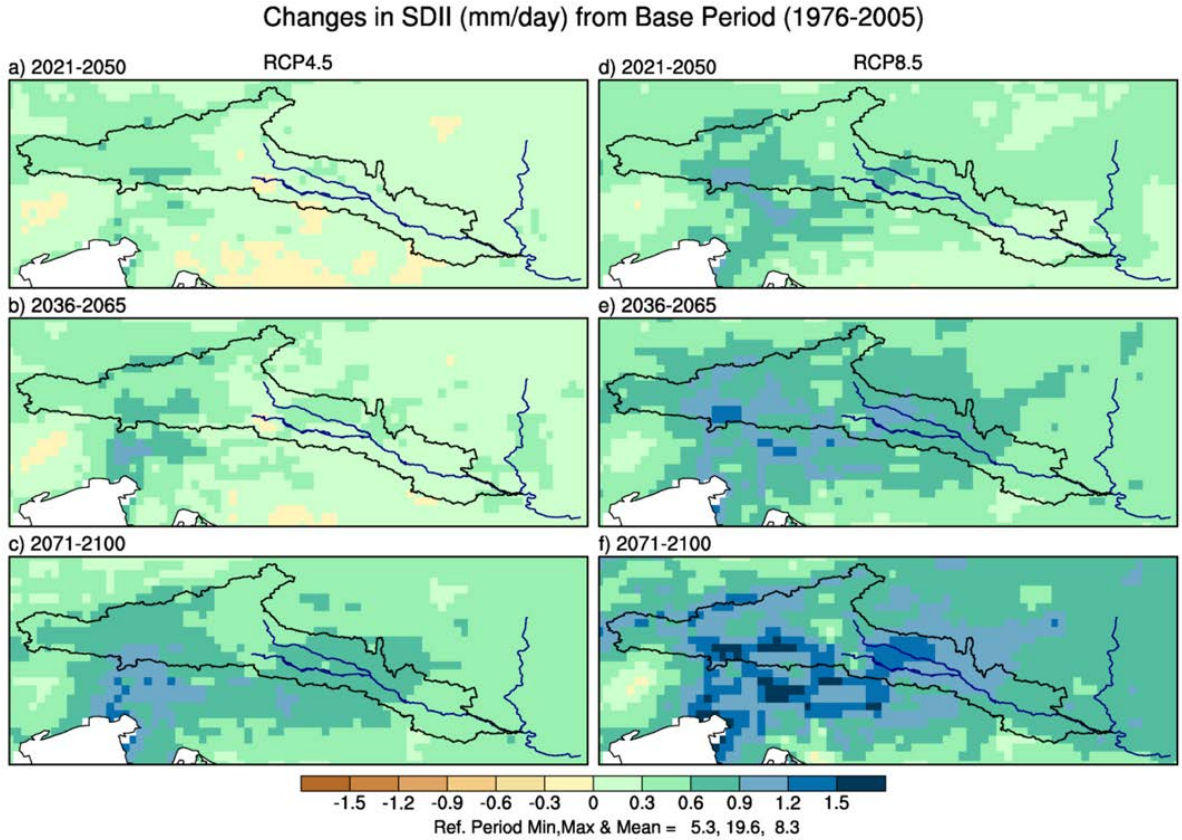

Figure 25 Differences in simple daily intensity index (SDII, See Table 3) using an ensemble mean of five selected models. The differences are taken by calculating the mean of each time-period mentioned in the panels against the mean of the reference period (1976-2005)

As shown in Table 3, we have also calculated the extreme indices for precipitation (RX1day, RX5day and PRCPTOT), but those are not presented in the main text. However, these indices are included in Appendix B. All those indices mainly point towards an increase in extreme precipitation events as we move towards the end of the century. In summary, based on the comprehensive analysis of climate extremes over the TBR MDD, we see a clear signal of increased heat related and intense precipitation events over the region throughout the century under emissions scenarios RCP4.5 and RCP8.5.

IV. Conclusions & Actions Recommendations

• Conclusions

In the present study, data from state-of-the-art regional climate models is used to quantify the impact of climate change under two emission scenarios on the TBR MDD region. The daily data from five most suitable regional climate models was bias-corrected using latest bias-correction methods against gridded observation, to correct biases in simulations and obtain simulated series with appropriate statistical properties. Based on bias-adjusted data, climate change analysis is done by plotting historical and future data in time series, box-and-whiskers and spatial plots. The results show a general warming and shifting precipitation patterns in changing climate. The summer months are projected to be 10% drier than during the reference period 1976-2005, and up to 20% wetter in winter months by the end of the century. Projections of temperature for all seasons show an increase in both minimum and maximum temperature with an average increase of mean winter (December-February) temperature up to 2.2°C till 2100 under RCP4.5 and around 4.2°C under RCP8.5 scenario. Such an increase can have possibly huge implications in areas with snow cover, reducing the availability of snow in winter and early snowmelt in spring, resulting in increased water stress later in summer months. Moreover, higher temperatures and decrease in precipitation during the prolonged vegetation period will lead to a general increase in water demand for agriculture and forestry in the study area. Without artificial irrigation the prolongation of the vegetation period will have no positive effects on agriculture. Reduction of river runoff in summer and increase in temperatures can significantly degrade the water quality. Such changes can result in shifts of some aquatic and terrestrial flora and fauna and hence affect the whole ecosystems and biodiversity of the region.

Our analysis of quantification of extreme indices shows a consistent increase in heat waves and intense precipitation events by the end of 21st century. Under both scenarios, all future time periods show increasing trends in summer days and tropical nights. The trend is stronger in hotter regions, which means the current hotter regions will experience even longer heat episodes in future. Increases in very hot summer days and tropical nights can lead to a rise in mortality as it makes it difficult for the human body to stay cool especially for sick and elderly people. Moreover, there is evidence of more warming being found in night-time (minimum) temperatures than in daytime (maximum) temperatures implying strong reduction of frost and ice days threatening the winter sports and tourism in the region. Precipitation-related indicators consistently predict an increase in heavy precipitation events in most of the region with the highest increase seen in Austrian Tyrol. Such an increase in frequency and intensity of extreme precipitation events is alarming as they are usually followed by heavy flooding events.

In general, projections for the TBR MDD under RCP4.5 and RCP8.5 emission scenarios show generally wetter conditions and higher flooding risks, but drier summer months.

- **Recommendations**

The present study is based on data from the five most suitable regional climate model simulations driven with data from global climate model (GCMs) of Coupled Model Intercomparison Project 5 (CMIP5). The CMIP5 model projections are based on 2100 radiative forcing values for four GHG concentration pathways called Representative Concentration Pathways (RCPs; van Vuuren et al., 2011). Recently, climate scientists have built a range of new "pathways" that include how global society, demographics and economics might change over the next century. These pathways are called "Shared Socioeconomic Pathways" (SSPs). The latest generation of global climate model simulations conducted under CMIP6 are based on SSP/RCP-based scenarios which combine SSP with the CMIP5 scenarios premises (RCP). The regional climate model simulation driven with CMIP6 GCM output is now underway in the CORDEX framework and the data from the latest generation of CMIP6 based RCMs will be available in coming years. It is highly recommended that future assessments of the climate change projections for the TBR MDD are based on a larger ensemble (at least 10 models) of CMIP6 based regional climate model simulations.

Our results show that climate change is inevitable and that there is an increasing need for adaptation and mitigation through cross-sectoral cooperation. Rehabilitation and restoration of rivers and floodplains in the TBR MDD region is vital and must be completed to mitigate the negative effects of both current and future climate change.

For successful climate change mitigation and adaptation in future, climate change research needs to be more transdisciplinary and integrative in future. We recommend some areas where climate change needs to be considered in adaptation and mitigation strategies to increase resilience against harmful impacts of CC:

- improved climate change projections, analyses, and assessments;
- safeguarding free-flowing rivers and restoring wetlands and floodplains to retain excess water is important to improve the state of water and ecosystem. The rivers impacted by dams or extensive development need more management interventions to protect ecosystems and people than basins with free-flowing rivers (Palmer et. al. 2008). As the lower Drava River Basin is one of the most extensively hydroelectrically exploited river basins in the world (Zakwan et. al. 2021), the river management and emergency action plans are particularly important in the TBR MDD to minimize dam-induced flood hazards.
- land-use planning that promotes plantation and development of agricultural land. As mentioned in a recent study by Kopsieker et. al. 2021, it is important to grow the most adapted trees in the right places where both climate and soil are suitable for the selected species. Moreover, river and floodplain rehabilitation and restoration have great potential to build resilience against floods;
- development of environmental research and information networks to exchange related climatological data about flood risks and mitigation planning, among the countries included in the TBR MDD;

- evaluation and analysis focused on measures of extreme events due to climate change, including flood vulnerability, to make the decision-making process more efficient and sustainable;
- improving existing flood alert systems, while also educating and training the local population, so that they are prepared to work on flood mitigation and to deal with other climate related hazards;
- align research goals with long term policies to build synergies across multiple objectives;
- designing a monitoring framework to enable adaptive management of the restoration trajectory.

V. References

A. Bronstert, V. Kolokotronis, D. Schwandt, H. Straub Comparison and evaluation of regional climate scenarios for hydrological impact analysis: general scheme and application example Int. J. Climatol., 27 (2007), pp. 1579-1594, 10.1002/joc.1621

Bisselink, B., Bernhard, J., Gelati, E., Jacobs, C., Adamovic, M., Mentaschi, L., Lavalle, C. and De Roo, A., Impact of a changing climate, land use, and water usage on water resources in the Danube river basin, EUR 29228 EN, Publications Office of the European Union, Luxembourg, 2018, ISBN 978-92-79-85888-8 (print),978-92-79-85889-5 (pdf), doi:10.2760/89828 (online),10.2760/561327 (print), JRC111817.

B. Klein, I. Lingemann, E. Nilson, P. Krahe, T. Maurer, H. Moser Key concepts for analysis of climate change impacts for river basin management in the River Danube River Syst., 20 (1–2) (2012), pp. 7-21

H. Li, J. Sheffield, E.F. Wood, Bias correction of monthly precipitation and temperature fields from Intergovernmental Panel on Climate Change AR4 models using equidistant quantile matching J. Geophys. Res., 115 (D10) (2010), pp. 985-993

Kopsieker, L., Costa Domingo, G., Underwood, E. (2021). Climate mitigation potential of large-scale restoration in Europe. Analysis of the climate mitigation potential of restoring habitats listed in Annex I of the Habitats Directive. Policy Report, Institute for European Environmental Policy.

Klein Tank, A. M. G., Wijngaard, J. B., Können, G. P., Böhm, R., & Demarée, G. (2002). Daily dataset of 20th-century surface air temperature and precipitation series for the European Climate Assessment. International Journal of Climatology, 22(12), 1441–1453.

Klein Tank et al. (2002) Daily dataset of 20th-century surface air temperature and precipitation series for the European Climate. Intern. J. Climatol. 22:1441-1453

Lazoglou, G.; Anagnostopoulou, C.; Skoulikaris, C.; Tolika, K. Bias Correction of Climate Model's Precipitation Using the Copula Method and Its Application in River Basin Simulation. Water 2019, 11, 600. https://doi.org/10.3390/w11030600

Lobanova, A., Liersch, S., Nunes, J.P., Didovets, I., Stagl, J., Huang, S., Koch, H., Rivas L´opez, Md.R., Maule, C.F., Hattermann, F., Krysanova, V., 2018. Hydrological impacts of moderate and high-end climate change across European river basins. J. Hydrol. Reg. Stud. 18, 15–30.

Lóczy D. (2019) Climate and Climate Change in the Drava-Mura Catchment. In: Lóczy D. (eds) The Drava River. Springer Geography. Springer, Cham. https://doi.org/10.1007/978-3-319-92816-6_4

Margaret A Palmer, Catherine A Reidy Liermann, Christer Nilsson, Martina Flörke, Joseph Alcamo, P Sam Lake, Nick Bond Climate change and the world's river basins: anticipating management options Front. Ecol. Environ., 6 (2) (2008), pp. 81-89

O'Neill BC, Kriegler E, Riahi K, et al (2014) A new scenario framework for climate change research: The concept of shared socioeconomic pathways. Climatic Change.
https://doi.org/10.1007/s10584-013-0905-2

Palmer MA, Reidy CA, Nilsson C, et al. 2008. Climate change and the world's river basins: anticipating management options. *Front Ecol Environ* 6: 81– 89

Pierce, D. D. R. Cayan, E. P. Maurer, J. T. Abatzoglou, and K. Hegewisch, Improved Bias Correction Techniques for Hydrological Simulations of Climate Change, Journal of Hydrometeorology, 16(6), 2421-2442, 2015.

Pongracz, R., Bartholy, J., Miklos, E. (2011), Analysis of projected climate change for Hungary using ENSEMBLES simulations. Applied Ecology and Environmental Research 9, 387-398.

R.C. Cornes, G. van der Schrier, E.J.M. van den Besselaar, P.D. Jones An ensemble version of the E-OBS temperature and precipitation data sets J. Geophys. Res. Atmos., 123 (2018), pp. 9391-9409

Renato Bertalanič, Mojca Dolinar, Luka Honzak, Neža Lokošek, Anže Medved, Gregor Vertačnik, Živa Vlahović 2019: Climate change projections for Slovenia over the 21st century: Temperature and precipitation summary Ljubljana, april 2019, Accessed Feb 2020: https://www.meteo.si/uploads/probase/www/climate/text/en/publications/OPS21_brosura_ENG.pdf

Stagl, Judith C., and Fred F. Hattermann. (2015). "Impacts of Climate Change on the Hydrological Regime of the Danube River and Its Tributaries Using an Ensemble of Climate Scenarios" Water 7, no. 11: 6139-6172

Stagl, J., Hattermann, F. F. (2015): Impacts of climate change on the hydrological regime of the Danube River and its tributaries using an ensemble of climate scenarios. - Water, 7, 11, 6139-6172. https://doi.org/10.3390/w7116139

Schneider, C., Laizé, C. L. R., Acreman, M. C., and Flörke, M.: How will climate change modify river flow regimes in Europe? Hydrol. Earth Syst. Sci. 17, 325–339, https://doi.org/10.5194/hess-17-325-2013, 2013.

S. Theobald, K. Träbing, K. Kehr, V. Aufenanger, M. Flörke, et al. ClimAware: impacts of climate change on water resources management. Regional strategies and European view. Final Report. [Research Report] irstea. 2014, pp.208. hal-02599772

van Vuuren, D.P., Riahi, K. The relationship between short-term emissions and long-term concentration targets. Climatic Change 104, 793–801 (2011). https://doi.org/10.1007/s10584-010-0004-6

van der Schrier, Gerard & National Center for Atmospheric Research Staff (Eds). Last modified 16 Dec 2019. "The Climate Data Guide: E-OBS: High-resolution gridded mean/max/min temperature, precipitation and sea level pressure for Europe & Northern Africa."

Zakwan Mohammad, Quoc Bao Pham, and Senlin Zhu. "Effective Discharge Computation In the Lower Drava River." *Hydrological sciences journal*, v. 66.5 pp. 826-837. doi: 10.1080/02626667.2021.1900853

VI. APPENDIX A

- **Supplementary figures for Climate Change Impact Assessment**

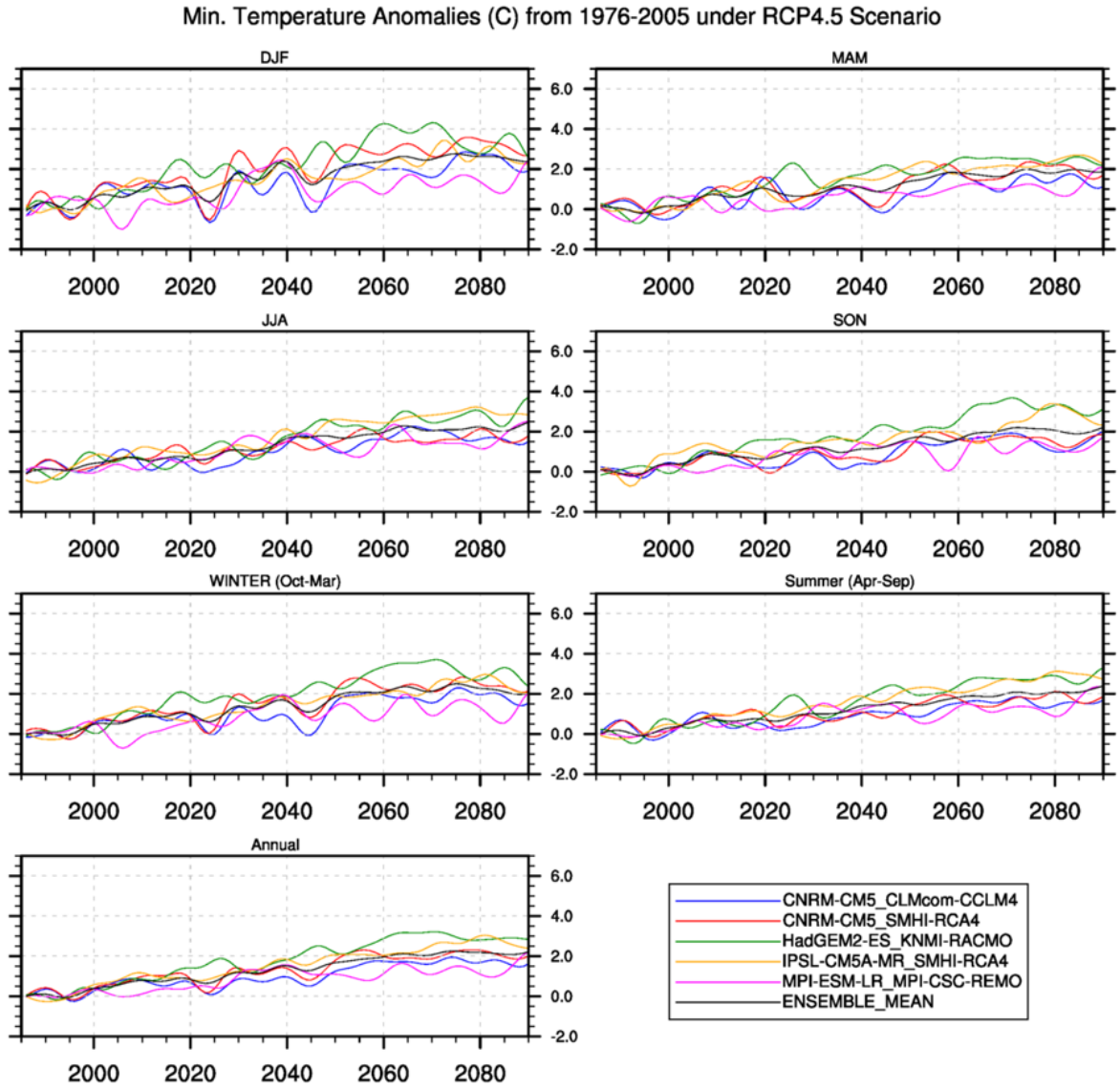

Figure A1 Average annual and seasonal anomalies of daily minimum temperature (in °C) from the base period 1976-2005 under RCP4.5

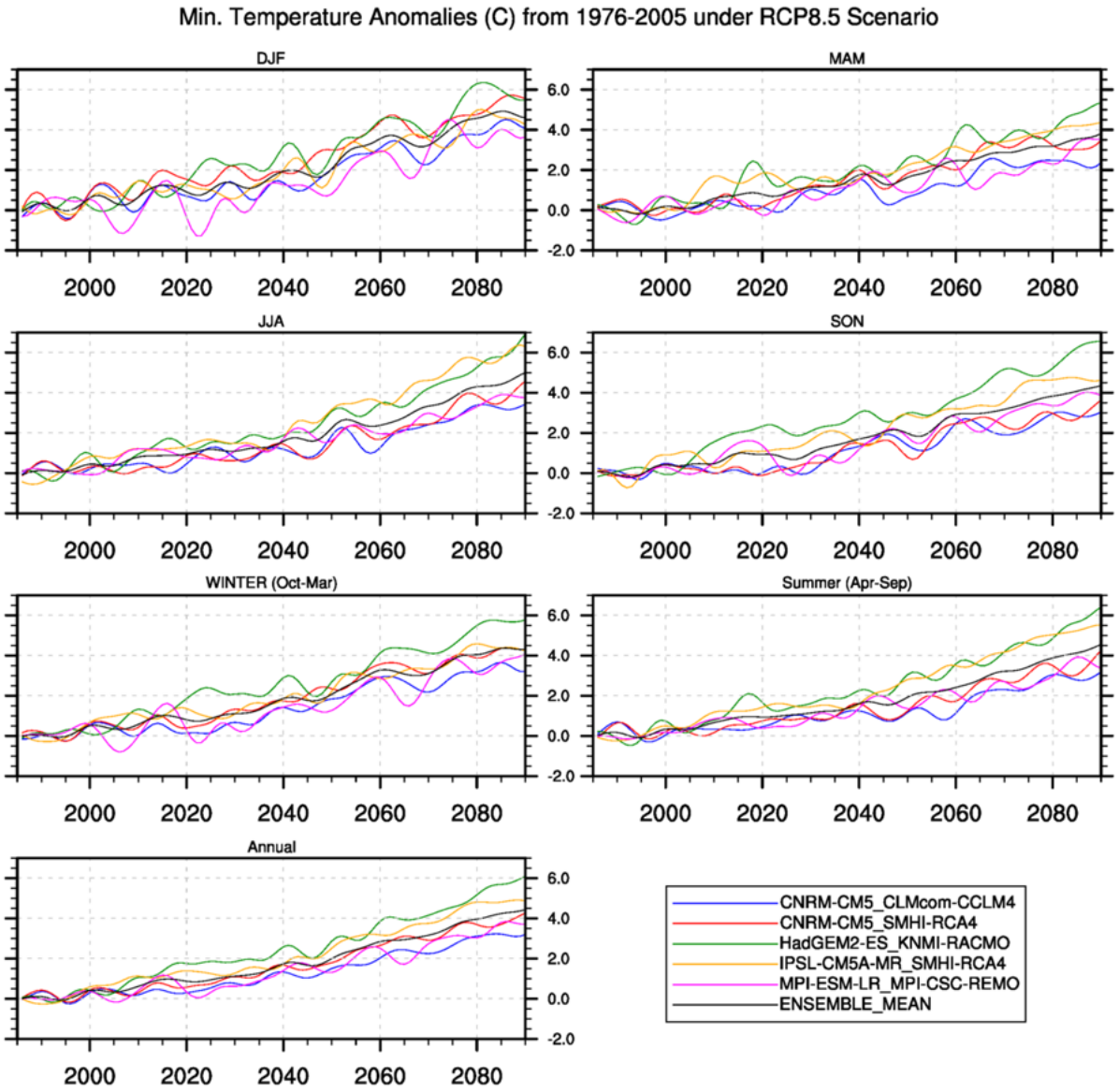

Figure A2 Average annual and seasonal anomalies of daily minimum temperature (in °C) from the base period 1976-2005 under RCP8.5

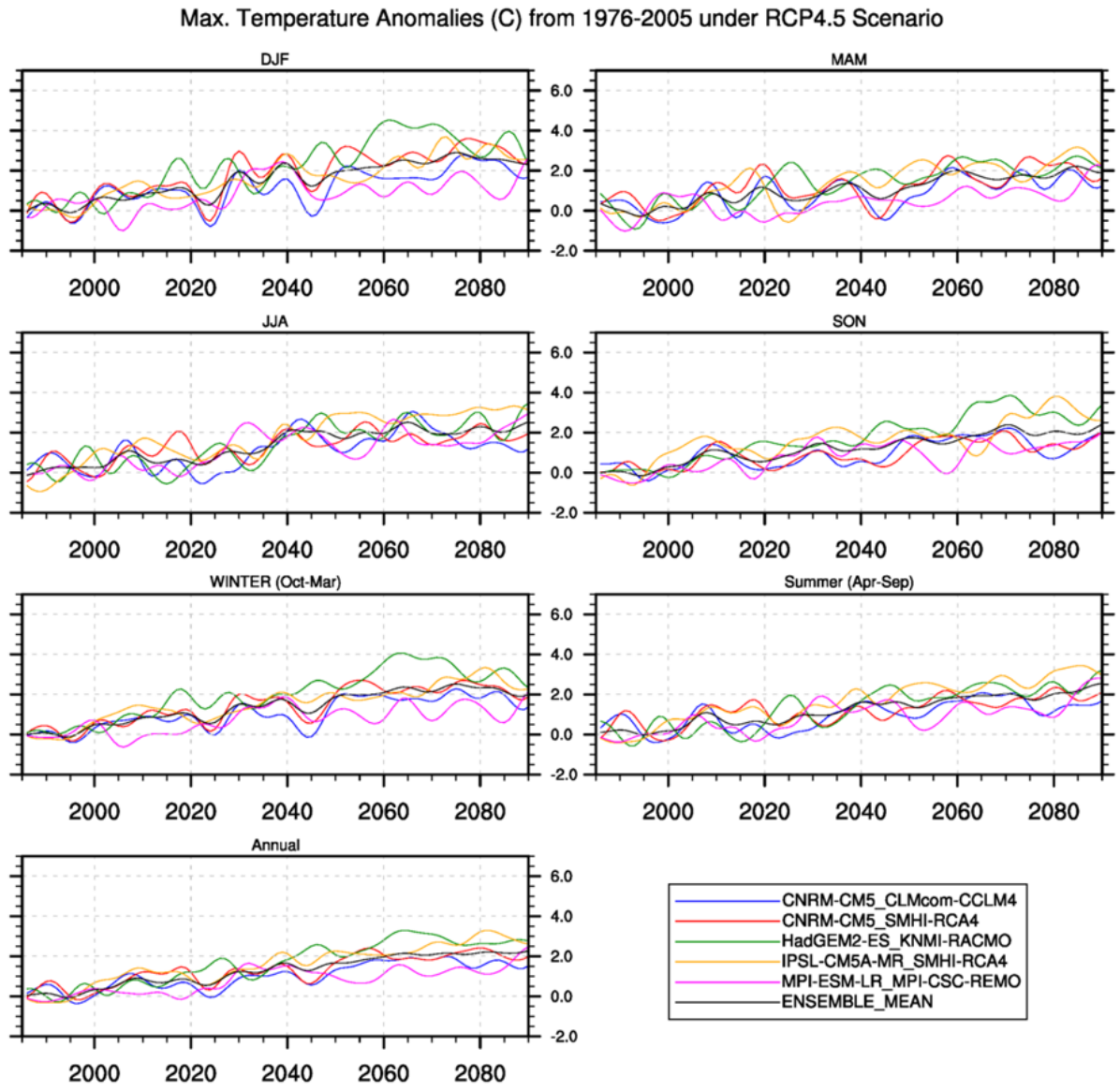

Figure A3 Average annual and seasonal anomalies of daily maximum temperature (in °C) from the base period 1976-2005 under RCP4.5

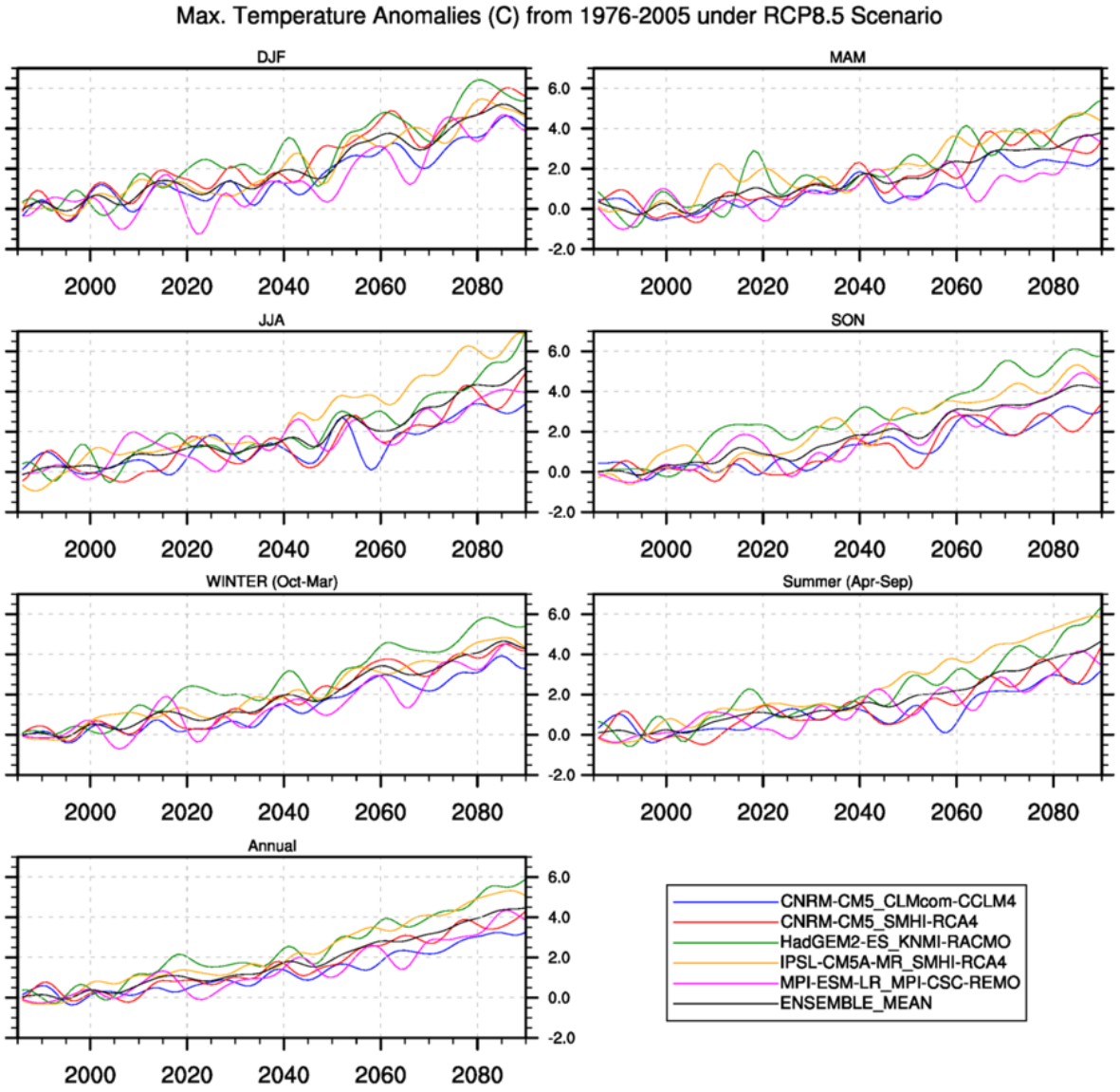

Figure A4 Average annual and seasonal anomalies of daily maximum temperature (in °C) from the base period 1976-2005 under RCP8.5

VII. APPENDIX B

- **Supplementary figures for Climate Extreme Indices Assessment**

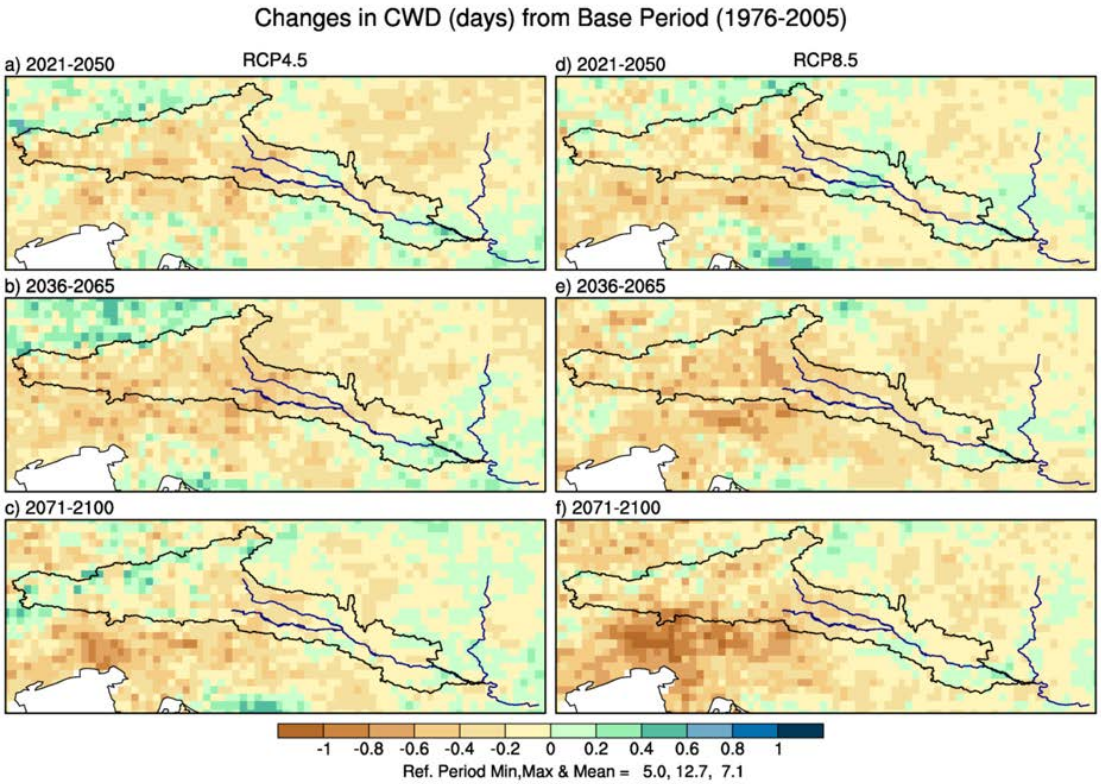

Figure B1 Differences in the number of consecutive wet days (annual) using an ensemble mean of five selected models. The differences are determined through calculating the means of each time-period and comparing them with the mean of the reference period (1976-2005)

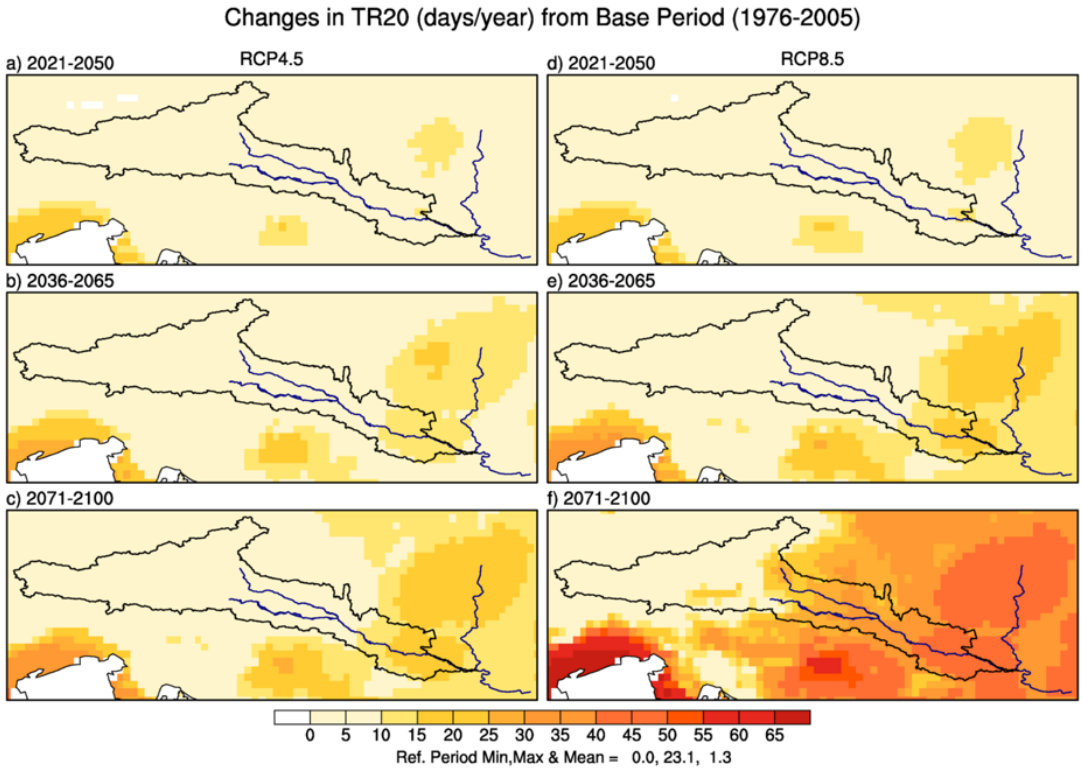

Figure B2 Differences in the number of tropical nights (TR20; Tmin > 20°C) using an ensemble mean of five selected models. The differences are determined through calculating the means of each time-period and comparing them with the mean of the reference period (1976-2005)

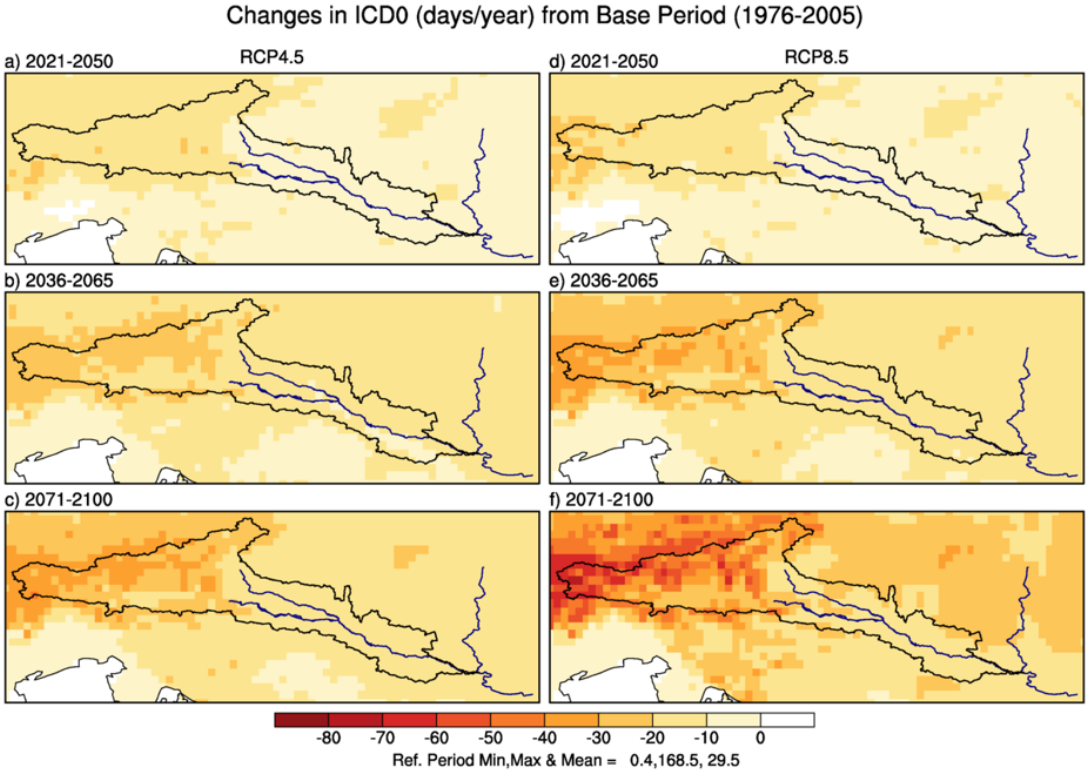

Figure B3 Differences in the number of ice days (ID0; Tmin < 0.0°C) using an ensemble mean of five selected models. The differences are determined through calculating the means of each time-period and comparing them with the mean of the reference period (1976-2005)

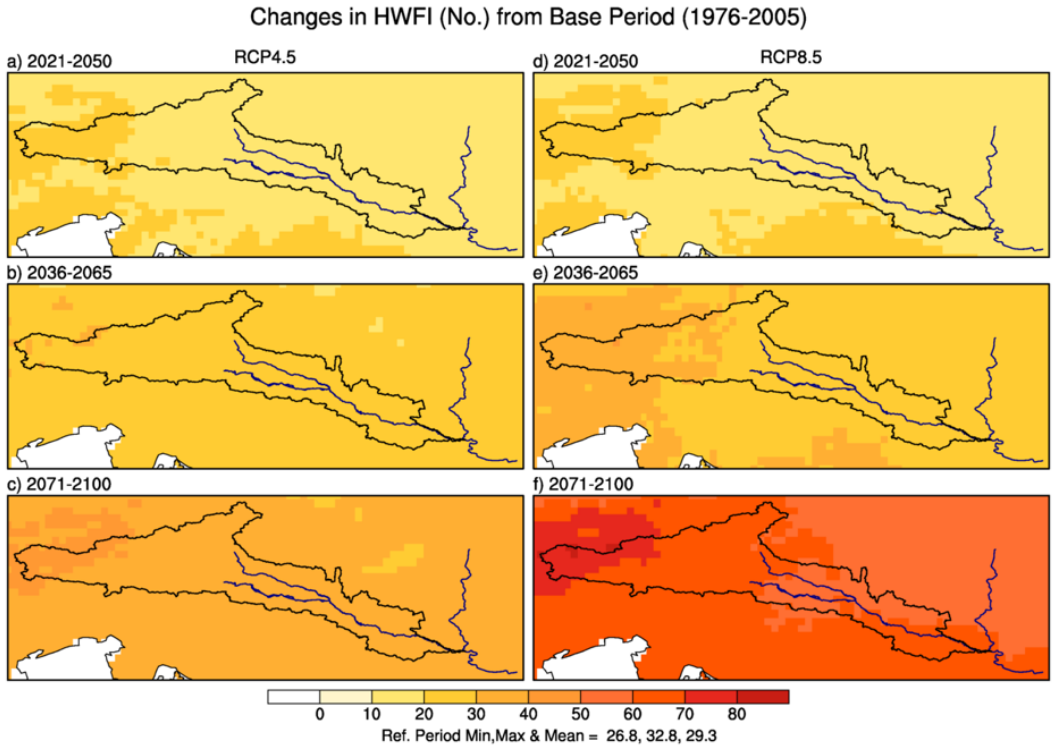

Figure B4 Differences in the heat wave frequency index (HWFI) using an ensemble mean of five selected models. The differences are determined through calculating the means of each time-period and comparing them with the mean of the reference period (1976-2005)

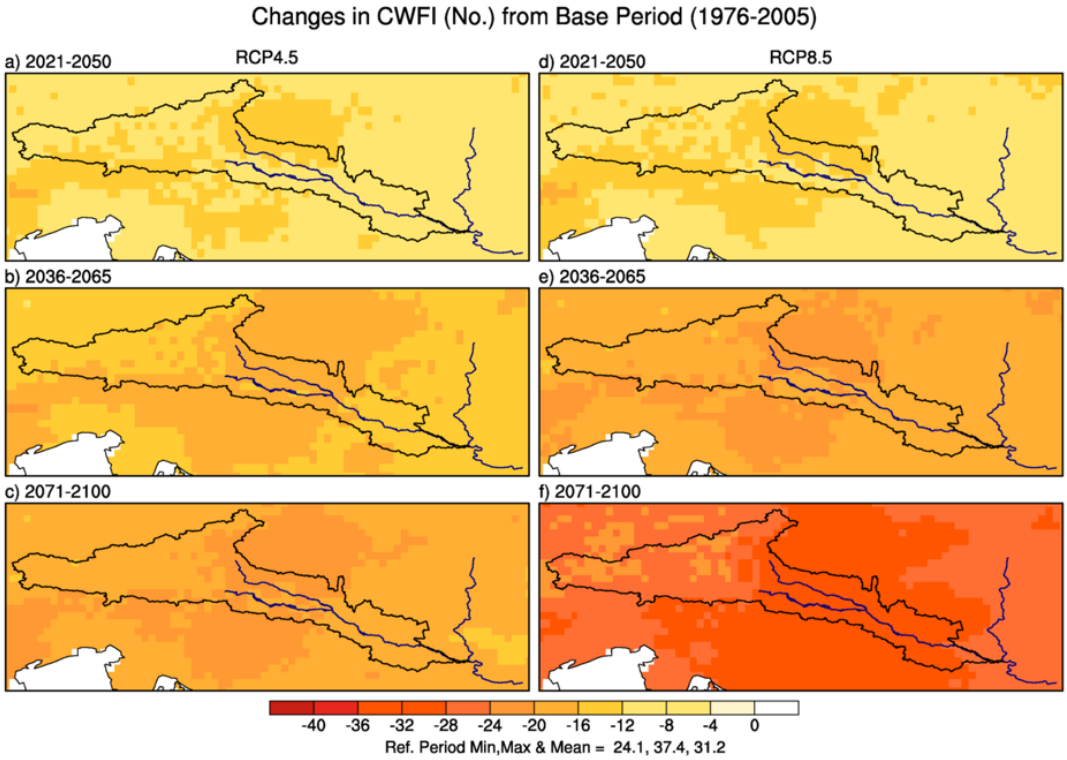

Figure B5 Differences in the cold wave frequency index (CWFI) using an ensemble mean of five selected models. The differences are determined through calculating the means of each time-period and comparing them with the mean of the reference period (1976-2005)

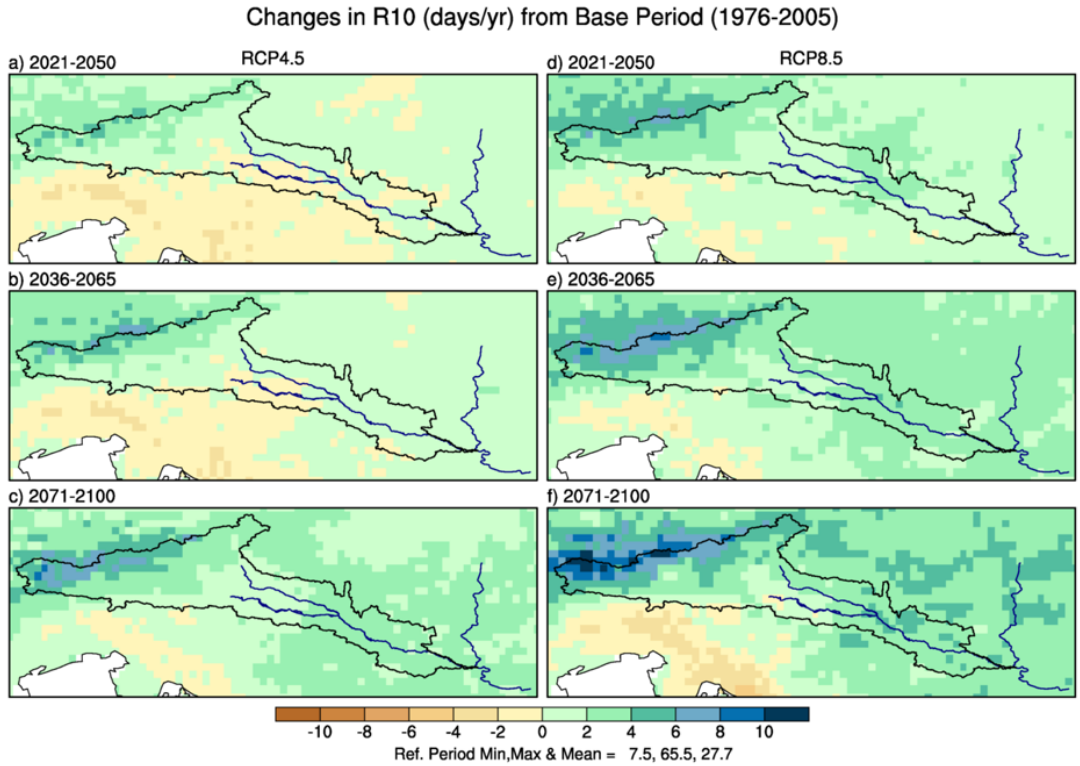

Figure B6 Differences in number of heavy precipitation days i.e., greater than 10mm symbolized by R10, using an ensemble mean of five selected models. The differences are determined through calculating the means of each time-period and comparing them with the mean of the reference period (1976-2005).

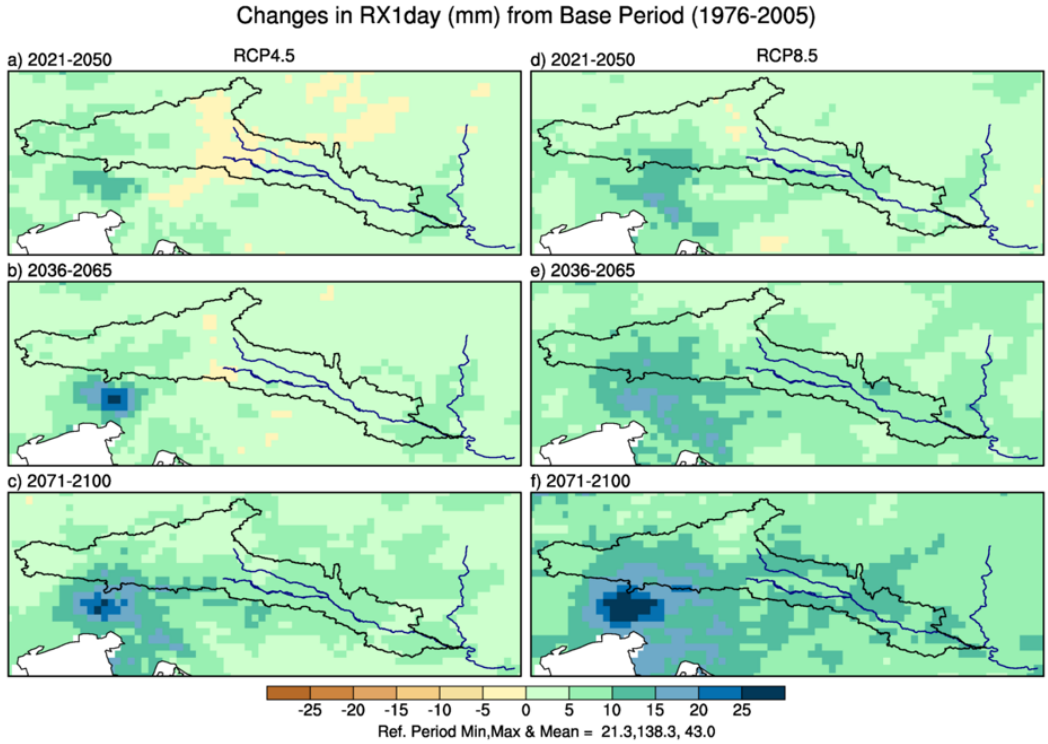

Figure B7 Changes in the maximum 1-day precipitation amount (RX1day) using an ensemble mean of five selected models. The differences are determined through calculating the means of each time-period and comparing them with the mean of the reference period (1976-2005)

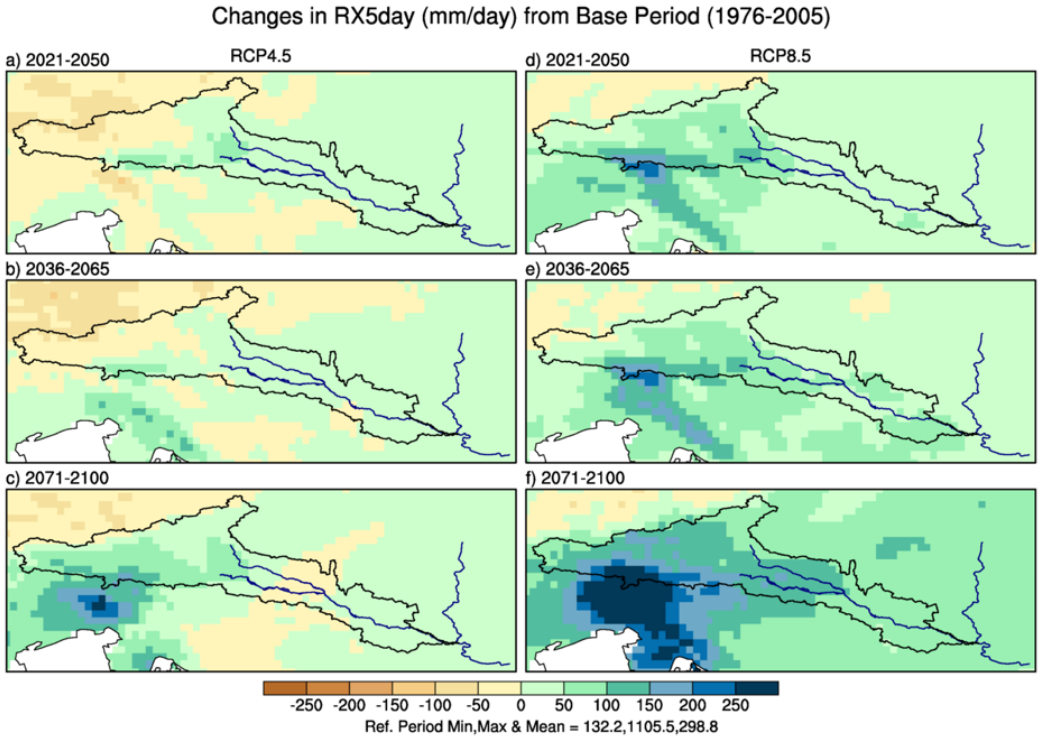

Figure B8 Changes in the maximum 5 days precipitation amount (RX5day) using an ensemble mean of five selected models. The differences are determined through calculating the means of each time-period and comparing them with the mean of the reference period (1976-2005).

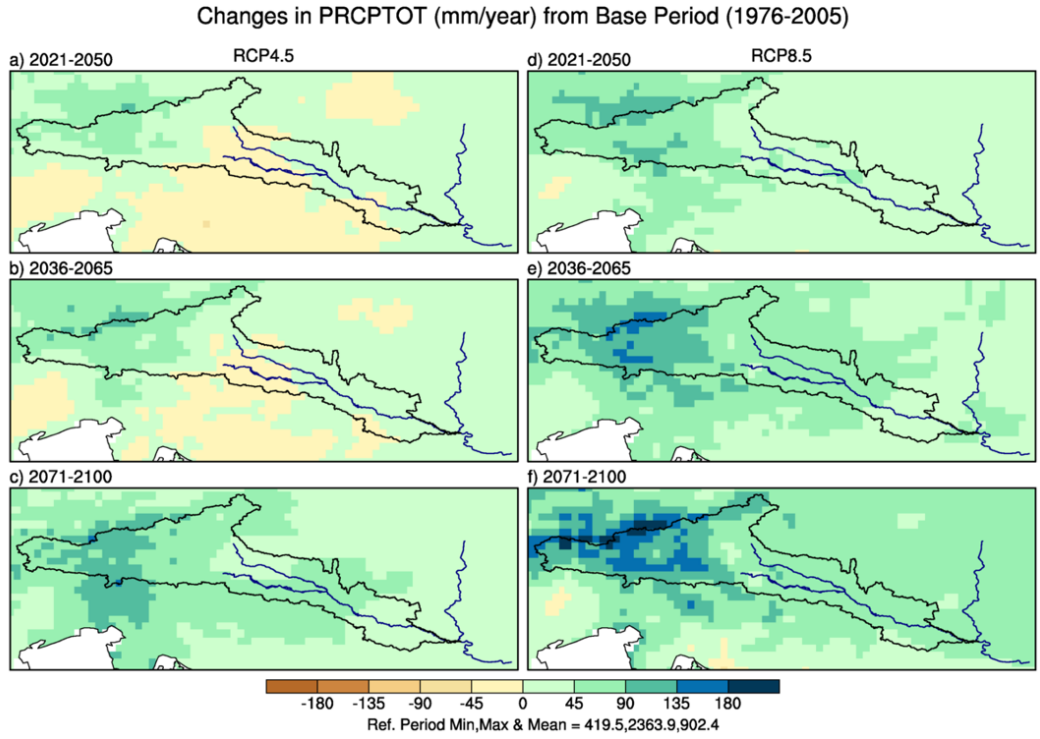

Figure B9 Changes in annual total precipitation of wet days (PRCPTOT) using an ensemble mean of five selected models. The differences are determined through calculating the means of each time-period and comparing them with the mean of the reference period (1976-2005)